Response to reviewer #2

We thank the reviewer for his thorough review and overview, and all his clarifying suggestions and comments. We address them below. We have marked the reviewers comment in black, and our responses in blue.

Interactive comment on "Surface velocity of the Northeast Greenland Ice Stream (NEGIS): Assessment of interior velocities derived from satellite data by GPS" by Christine S. Hvidberg et al.

Martin Lüthi (Referee)

General assessment:

This is a very interesting manuscript describing a unique data set on the ice motion in the interior of the Greenland Ice Sheet. The paper shows many interesting observations, and provides an extremely useful assessment on the accuracy of remote-sensing products. That being said, the focus of the publication is not entirely clear. There is some glaciology, but the major part is dedicated to the data products comparison. Since all of this hinges on the GPS measurements, this is not a problem, but maybe this should be made more clear by the structure of the paper.

Most parts read nicely, but especially towards the end (Discussion and Conclusions) it seems that the paper was hastily thrown together without much proofreading, or streamlining. So, theses sections merit some more effort, mostly structurally and cosmetically.

Response: We have restructured the results and discussion sections slightly according to the suggestions by reviewer #2. We agree with the editor on his suggestions, and find that the structure is now more clear and with an improved logical flow.

We have divided the section presenting the comparison with satellite-derived products into two sections 3+4: section 3 presents the satellite data products, and section 4 presents the comparison with GPS data. In the discussion section, the last subsection 5.4 about flowlines is now reordered to be section 5.2 and the flowline calculation is now introduced as part of the assessment in section 4. We have rewritten the last part of the conclusion.

Also the abstract is longish and should be somewhat condensed.

Response: We have shortened the abstract from 302 words to 259 words.

Most figures also deserve some more love. Why is Figure 1 just a gray blob? Also a inset with the part of Greenland depicted is missing. Figure 3, which is central, should be much improved, mainly with less axes and larger content. Also Figure 6 seems to be a mixture of Excel with some random typesetting for the numbers, and should be redrawn.

Response: We have revised figures 1, 3, 4, 6, 7 (now 8) according to the suggestions by reviewer #2. In figures 2 and 7 we added titles to colorbars as suggested by reviewer #1. We have explained all the revisions in the points below, and we agree that figures 1 and 3 in particular, are now improved.

Overall, this is a very interesting study, that I recommend for publication after the points below have been addressed.

Thank you.

We have explained below how we address the points:

16 is this the coordinate of the site, or of EastGrip? Anyway, this should not be in the abstract

Response: We mentioned the coordinates of the EastGRIP site. We have removed the coordinates from the abstract. We mention the coordinates again in the last paragraph of the introduction and in the section 2.1 on the GPS stake network. Both places we have revised to clarify that the coordinates now mark the central reference stake of the GPS network, located 300 m from the EGRIP deep drilling site.

19 transverse strain rates? or longitudinal? please specify

Reponse: both, we have added “longitudinal and transverse”

43 coordinates could be given here

Response: as mentioned above, we have mentioned the coordinates in introduction and in the section 2.1 along with the description of the GPS stake network.

49 "induces"

Corrected, thank you.

55 the measurement site coordinates should be given here. This is more important than the coordinates of the EastGRIP field site, which can be looked up if needed. OK, after reading on, I see in Figure 2 that the EastGRIP site is the central site of the GPS network. This should be mentioned here, and in the abstract.

Response: we agree with the reviewer that this should be specified clearly. As explained above, we removed the EGRIP coordinates from the abstract.

In the introductory paragraph we inserted the following text and removed the coordinates of the EGRIP deep drilling site: “… and centered around a reference stake (75°38’ N, 35°58’ W) located 300 m from the East Greenland Ice-core Project (EastGRIP) deep drilling site.”

In the description of the GPS stake network, we inserted similar text and removed the coordinates of the EGRIP site: “…, including a central reference stake (75°38’ N, 35°58’ W) located 300 m from the EastGRIP deep drilling site,… “

57 better called "elevation model"

Done

75 I do not see any topographic undulation in Figure 2. Indicate which panel, and what to look for.

Response: We agree with the reviewer that it is a little difficult to identify the undulation. We revised and added some explanation in the brackets with the reference to the figure: “across a topographic surface undulation northwest of NEGIS (a 20-30 km wide dark/bright pattern perpendicular to NEGIS, Fig. 2a).”

A note: the topographic undulation of the surface is related to large undulations in the internal radar layers within the ice (unpublished work), and we are investigating the origin of these internal layer undulations.

79 "which were drilled..."

OK, corrected

80 Why was there no local GPS reference at EastGRIP wchich seems mandatory for meaningful strain measurements. additionally: was there any GPS station running continuously to assess seasonal or episodic changes in flow velocity?

Response: We have installed a reference station in the center of the stake network, and it is included in the analysis. The reference station was observed for extended multiple periods each season, but we have not had the reference station running continuously throughout the years. We have used the station to assess our PPP processing results and estimate the uncertainties. We explain this in our response to reviewer #1, and as explained in the response we have added some text to explain this in more detail:

“The PPP approach can introduce systematic errors if the stake is moving (King, 2004). To optimize our processing protocol and evaluate timing estimates and position uncertainties, we observed the central reference stake at the EastGRIP site (red dot in Fig. 2) over extended periods each season and compared separate 1-hour static, 24-hour static, and kinematic solutions. We found that the 24-h static solution performed better than the average position of a 24-hour kinematic solution. With a maximum observed surface speed of approximately 60 m a^{-1}, the uncertainty related to the static solution is estimated to be < 2 cm. We estimate the combined uncertainty of our GPS positions to be within 3 cm.”

We did not identify any episodic changes in ice flow velocity in our data so far. This was also not expected since our site is located far inland and surface velocities are 1-2 orders of magnitude lower than in the fast outlets. However, in future work we will investigate the observations from the reference stake further, together with similar observations over extended periods from the stake located 25 km downstream from EGRIP. Since almost all of our stakes are only observed annually, our data would not resolve seasonal variability in the flow of these stakes.

105 this sounds overly optimisitc, since the stake tilt was not measured.

Response (same as to reviewer #1): we have no precise observations of the tilt or changes in tilt over time, unfortunately. We have only been able to correct for the tilt in our processing. As explained in the text, our linear fit included fitting an unknown displacement at the time when/if the stake was extended, and this displacement is interpreted as a small tilt of the stake. We assume that the tilt did not change over time, and we believe that it is realistic that the stakes could have been installed with a small tilt, or that the extension of the stake was slightly tilting. We assess that changes in tilt over time are negligible compared to other uncertainties.

We revise the text “A possible small tilt of the stake can lead to uncertainties in the horizontal position. We take this into account by including an unknown horizontal shift in the position of stakes that were vertically extended.” To be: “A small tilt of the stake can lead to uncertainties in the horizontal velocity. We take this into account by including an unknown horizontal shift in the position of stakes that were vertically extended, and we neglect any other changes in the tilt.”

106 there seems to be the tacid assumption of steady flow without seasonal or episodic variablility. If so, make this statement very clearly.

Response: we add the following to the first sentence “…, assuming a constant displacement rate.”

109 this is maybe the statement I asked about on line 106. But then this should be "displacement rate", i.e. velocity

Done, see response above.

117 spell out "Figure 2" in the running text, and abbreviate in parentheses (according to the journal style)

Reponse: Thank you. This is corrected throughout the paper.

119 leave away "see" in figure references (please change everywhere). Also, I would put these references in the running text, since these are important major results of the study.

Response: Corrected, and changed throughout the paper.

121 use words for ">", e.g. "for a flow band wider than 10 km"

Done. Also changed at a few other locations in the paper.

121 abbreviate "meter" to "m" (SI units)

Done

127 "a linear velocity field"

OK, added "field".

130 maybe qualify "horizontal compression" etc.

Done

131 should be "oriented at" (typo)

Corrected

141 "Figure 3b"

Corrected

141 "horizontal shear strain rate" (also 146)

Corrected

144 "Figure S1"

Corrected

187 Also say "Sentiel 1-A/B" (like ENVEO) (also 193)

Done

193 why is [Strozzi] in square brackets??

Corrected to ().

196 Use just one way writing Sentinel-1A/B

OK, corrected

205 It would be useful to clearly state products developed by the authors, as opposed to products from other groups. 7) seems to be one of them (?)

Response: Products from sources no. 5), 6) and 7) were developed by the authors. Products from sources no. 6), 7) and 8) are considered "experimental products", and this is mentioned in the manuscript. Products from source 5) are available for download through the PROMICE site. A new reference with description of product no. 6) has been added (Andersen et al., 2020). The product no. 7) is described here, and not published elsewhere. We believe that products 5) and 6) are sufficiently referenced, but we agree that it would be useful to explicitly mention that the product 7) is not presented elsewhere.

We have therefore added the following remark after presenting the products from source 7): “The product from AWI-TSX product was developed for this study.”

A new reference for product 6) is inserted:

Andersen, J. K., A. Kusk, J. P. M. Boncori, C. S. Hvidberg, A. Grinsted: Improved Ice Velocity Measurements with Sentinel-1 TOPS Interferometry. Remote Sensing, 12(12), [2014]. https://doi.org/10.3390/rs12122014, 2020.

216 8) is quite confusing, as it starts with Measures, but the the description changes to "we"

Response: As mentioned in the beginning of the section, we calculate long-term averages for each type of product. For product 8), we explain that we derive two long-term average products. We agree with the reviewer that the text could be a little more clear. We have moved our explanation of the two long-term products to the end of the paragraph and slightly revised by starting with “For the assessment here…” instead of just “Here”. We also add a sentence at the end: “These two products were included in the assessment.”

227 It would be helpful to add a subsection here: "Assessment" and one before the product description starts: "Data products" or "Data sources" or similar.

We have added a new section 4 with the assessments, containing two subsections, one with the ArcticDEM and one with the velocities. The product descriptions are now in a separate section 3, also containing two subsections, one presenting the ArcticDEM and one presenting the velocity products. This seems to greatly improve the structure, thank you for the suggestion.

228 well, we could argue that also GPS is "satellite-based"

Response: Yes, GPS is satellite based, but the GPS derived velocities are not generally known as being satellite-based. We noticed that we use the expressions satellite-derived and satellite-based inconsistently. We have now changed throughout the manuscript to use the terms: “satellite-derived velocities” and “GPS derived velocities”, and similar for strain rates. So we completely removed the expression “satellite-based”.

234 "minimizes"

OK, corrected.

236 "Figure 6" (also 241...)

OK, corrected Fig. to Figure.

250 "provides"

OK, corrected

260 you say "Both", but list three products: clarify!

Response: we only mention two products in this paragraph, but the AWI-TSX product is mentioned twice. We have slightly revised the paragraph to make it more clear.

262 "Measures" twice

OK, we have revised the sentence.

273ff this section is the textual representation of the table, and therefore unreadable, the second part repeats the section before -> delete are streamline considerably

Response: We agree that the product names are complicated, and it is difficult to read the text with all these products mentioned. On the other hand, we also find it useful to mention and briefly evaluate each of the top products. The five products with minimum bias are not shown in the main article, only in the supplementary material (The table in the main article is sorted after rms precision), so we find that it is useful to mention these numbers, and it helps reach the conclusion about the SAR based products. We have revised the section with a discussion of the derived flowlines, and we now refer back to the products with a low bias. Therefore, we keep this list of products with their bias in the first part of the paragraph.

The sentence about the DTU-Space product was partly repeated from the paragraph above and is now shortened down to: "Of these, the DTU-Space-S1 product stands out ~~with its short temporal coverage, low standard deviation and low optimal smoothing length~~ *as mentioned above*".

290 should this be "SAR speckle tracking" (since all products use SAR)

Response: We revised to "SAR speckle tracking products" for clarification.

292 "comparably"

OK, corrected.

296 "errors" instead of "uncertainties"

OK, revised

302 "Fig. 4" (capitalize)

Done

305 This is a somewhat overly enthusiastic conclusion. If the velocity errors are of the same magnitude as the signal (outside the fast-flowing area) there are severe limitations on the usefulness of the products. I think that relative errors should also be discussed.

Response: We agree that this text could be more precise. We have revised the first paragraph of section 5.3. We revise the text from:

"The assessment of satellite-based velocity and height products provides confidence in the satellite-based products in the interior regions of the Greenland ice sheets. Thereby, it enables us to use the GPS derived velocities and strain rates in combination with satellite-based data to characterize spatial patterns in surface structure and ice flow in the interior part of the NEGIS ice stream."

The text is revised to be:

"The assessment of satellite-derived velocity and height products inform of the accuracy and limitations of the satellite-derived products in the interior regions of the Greenland Ice Sheet. In our study area the best products have a bias and precision of less than approximately 0.5 m a^{-1}, i.e. about 5% of the smallest observed GPS derived velocities of around 10 m a^{-1}. Knowing the limitations of the satellite-derived products, we are now able to combine the GPS derived velocities and strain rates with satellite-derived data to characterize spatial patterns in surface structure and ice flow in the interior part of the NEGIS ice stream. We discuss here the observed patterns."

315 "by an order of magnitude"

OK, corrected

316 "remarkably uniform"

OK, corrected

317 "support the notion of" (I don't think you talk about the process here)

Response: We agree that the text is a little unclear here, and reviewer #1 also pointed this out.

We sentence is changed to: "The remarkably uniform velocities and low strain rates in the fast flowing central band of NEGIS with narrow shear zones at the margins with enhanced strain rates is characteristic of ice stream flow (e.g. Minchew et al., 2018). In our study area in NEGIS, Holschuh et al. (2019) proposed that thermal softening of ice is present in the shear margins, despite the relatively low strain rates."

319 "an ... troughs" is inconsistent

Response: Ok, we can see that it is inconsistent. The text has been revised to be: "The surface topography reveals a 30-40 m deep lowering coinciding with the fast flow within NEGIS with well-defined deep troughs marking the shear margins."

320 compression would lead to ridges, so its likely extension due to flow acceleration, or side shear

Response: We removed "transverse compression"

321 "at an angle of"

Corrected

356 These are important points, but I did not see any assessment of the flow direction derived from different products... (a next paper?) Oh, I see you do exactly that, but these results (Figure 8) should probably be part of the comparison section. In any case Fig. 8 should be featured more prominently, and here the results should be discussed (but presented earlier).

Response: Thank you to the reviewer for this suggestion. We have now moved the presentation of the derived flowlines in figure 8 (now figure 7) up to the section 4.2 with the assessment of the velocity products. We insert the following paragraph at the end of section 4.2:

"As part of the assessment, we use the whole set of satellite-derived surface velocity products to trace flow lines along NEGIS. We use a starting point at the central reference stake near the EastGRIP site, which is located in the center of our observed area in a relatively narrow section of the NEGIS ice stream. We trace the flow lines upstream into the slower moving areas where flow converges into NEGIS and downstream into faster flow where the ice stream widens (Fig. 7). The flow lines are gradually displaced depending on their bias and fluctuate depending on their standard deviation. "

Also, we have reordered the subsections of the discussion to underline that this discussion belongs to the assessment, and the section discussing these flowlines are now placed immediately after the discussion of the satellite products, i.e. subsection 5.4 is now 5.2. The text is slightly revised to take into account that the figure is introduced earlier. We also inserted a sentence to stress that a low bias is needed to obtain reliable flowlines: "The flowlines for the products with minimum bias are marked (Fig. 7), showing that flowlines can only be reliably traced if the bias is small."

365 Twice northeast in the same sentence. The Conclusions seem to be hastily written, but should be carefully crafted.

Response: We have revised the first sentence to avoid using northeast twice. We have added a new paragraph at the end of the conclusion as explained in the points below.

368 "drop"

OK, corrected

392 "investigated" (everything else is written in the past tense) Also this paragraphs starts out of nowhere, like just thrown in hastily before submission.

Response: We have completely rewritten the last paragraph of the conclusion. We now focus on the uncertainty of the satellite-derived velocities, and we end with a conclusion regarding these products and their use for wider glaciological applications.

The last three paragraphs are now:

"The assessment inform of the accuracy of the satellite-derived velocities, and thereby allow us to evaluate the use of these products for investigations of flow patterns in the interior regions of the Greenland Ice Sheet. We show that satellite-derived strain rates can capture high-resolution spatial signals at the shear margins and within the fast flowing part of NEGIS, despite the high uncertainty in the order of 10^{-3} a^{-1}. We show further that the strain rate peaks along NEGIS are part of a regular undulating pattern forming in surface slope and strain rates when the surface velocity exceeds approximately 55 m a^{-1}, and we argue that the formation of these undulations appears to be related to bedrock topography.

We derived flowlines from the satellite-derived velocity products and showed that even a minor bias in these products can severely affect the path of the flowlines, in particular in slow-moving areas. We conclude that reliable flowlines can only be derived from satellite-derived velocities with a low bias of less than 1% compared to the surface speed, and that surface slopes may produce more realistic flowlines than satellite-derived velocities in slow-moving areas.

The study demonstrates that it is important to know the limitations of the satellite-derived products. We conclude that available satellite-derived products are sufficiently accurate to allow a detailed analysis of the ice flow in the interior part of NEGIS, which can contribute to understand the flow near its onset in interior North Greenland, and ultimately to improve projections of its future response to mass loss at the margins. "

396 A nice, general concluding statement would round off the paper better.

Done, see inserted text above

569 Caption should start right away (leave away "This table shows...")

OK, corrected

Fig 1 would be better in color. Also it should contain an inset map of Greenland, since not everybody knows where NEGIS is

Response: OK, done. We have inserted a map and changed to color.

Fig 2 the black line of panel B should be shown in panel A for comparison.

Response: The black line is not added because it disturbs the overview of the stake network and GPS velocities The line is shown in panel B along with the stakes and transverse lines.

Panel A: Giving the heights in a greyscale map is not very useful. Better plot the points on a hillshade with suitable lighting. Alternatively use a high-contrast color map for the topography. The red dot is not visible under the red arrow. Different color and Diamond shape would help

Response: We can see what the reviewer mean, however we think it is good to see the real surface elevation map, and not a hillshade. We have inserted a reference to figure 8 (previously figure 7), where the same area is shown with elevation and surface slopes in colormap, and with the black line indicated.

Fig 3 This figure is central to the paper, and should therefore be crafted with care. Could the panels be better combined such that the content is bigger and the labels appear only where needed? E.g. distance along profile and surface elevation is the same for all panels and should only appear at the bottom and at right.

Response: we have reduced the spacing between the panels and removed labels, so they only appear once for each coloumn/row. We have added a line to indicate the position of the reference stake in the b) transect.

panel f (bedrock): please indicated *measured* bedrock depths at crossing profiles from Icebridge, seismic soundings, radar. Also indicate the position of the borehole in panels d-f. [Morlighem is nice, but is heavily interpolated and is off by hundreds meters in places, depending on his assumptions on ice flow]

This point belongs to figure 4 and is addressed below.

Response: we agree with the reviewer that the interpolated bedrock maps are

Fig 4 combine the plots with (sharex: looks like matplotlib) for better visibility vertical dotted or very thin linkes would be useful

Done

panel f (bedrock): please indicated *measured* bedrock depths at crossing profiles from Icebridge, seismic soundings, radar. Also indicate the position of the borehole in all panels, but especially here. [Morlighem is nice, but is heavily interpolated and might be off by hundreds meters, depending on assumptions on ice flow]

Response: We indicate the position of the bore hole with a gray vertical line. We did not include any radar observations of bedrock depths in this paper. We refer to a new paper presenting some of these data (Franke et al. 2020), but our focus here is on the surface velocities and GPS, and including all the available radar data is outside the scope of this paper.

Fig 5 caption (last sentence) "Figure 3b" I don't know what the yellow dots mean, I don't see any in Fig. 3

Response: The yellow dots are seen in figure 5 and indicate the three stakes, where we calculated strain rates. We clarified the text and removed the reference to figure 3.

Fig 6 Why is the plotting style so different? Gray background does not help readability and should be changed to white (like all other Figs)

Response: We have made a new version of this figure. The background is white with black margins.

label the panels with a), b), c) and adjust the caption Why are these graphs on a logarithmic scale (vertically)?

Response: We have labeled panels a) to c). We used logarithmic sales horizontally because of the huge spread in temporal coverage from 6 days to decades, and vertically because we wanted to emphasize the decreasing relationship with increasing temporal coverage.

References: For quite a few papers the DOIs are missing.

OK, all are inserted (except one which is not available)

We include below a revised version of the manuscript with marked track-changes according to the suggestions by both reviewer #1 and #2.

Surface velocity of the Northeast Greenland Ice Stream (NEGIS): Assessment of interior velocities derived from satellite data by GPS

Christine S. Hvidberg[1], Aslak Grinsted[1], Dorthe Dahl-Jensen[1], Shfaqat Abbas Khan[2], Anders Kusk[2], Jonas Kvist Andersen[2], Niklas Neckel[3], Anne Solgaard[4], Nanna B. Karlsson[4], Helle Astrid Kjær[1], Paul Vallelonga[1].

[1]Niels Bohr Institute, University of Copenhagen, Copenhagen, Denmark.
[2]DTU-Space, Technical University of Denmark, Kgs. Lyngby, Denmark.
[3]Alfred-Wegener-Institut, Helmholtz-Zentrum für Polar- und Meeresforschung, Bremerhaven, Germany.
[4]Geological Survey of Denmark and Greenland, Copenhagen, Denmark.

Correspondence to: Christine S. Hvidberg (ch@nbi.ku.dk)

Abstract. The Northeast Greenland Ice Stream (NEGIS) extends around 600 km upstream from the coast to its onset near the ice divide in interior Greenland. Several maps of surface velocity and topography in the interior Greenland exist, but their accuracy is not well constrained by in situ observations~~ and limiting detailed studies of flow structures and shear margins near the onset of NEGIS~~. Here we present the results from a GPS mapping of surface velocity in an area located approximately 150 km from the ice divide near the East Greenland Ice-core Project (EastGRIP) deep drilling site~~ (75°38' N, 35°60' W)~~. A GPS strain net consisting of 63 poles was established and observed over the years 2015-2019. The strain net covers an area of 35 km by~~along NEGIS and~~ 40 km~~ across NEGIS~~, including both shear margins. The ice flows with a uniform surface speed of approximately 55 m a^{-1} within a central flow band~~>10 km wide central flow band~~ with longitudinal and transverse strain rates in the order of 10^{-4} a^{-1}~~.~~ and increasing by an order of magnitude~~The strain rates increase~~ in the shear margins~~ by an order of magnitude, and 10-20 m deep shear margin troughs mark a zone with enhanced longitudinal stretching, transverse compression and shear~~. We compare the GPS results to the Arctic Digital Elevation Model~~ (ArcticDEM)~~ and a list of satellite-derived~~based~~ surface velocity products in order to evaluate these products. For each velocity product, we determine the bias and precision of the velocity compared to the GPS observations, as well as the smoothing of the velocity products needed to obtain optimal precision. The best products have a bias and a precision of ~0.5 m a^{-1}. We combine the GPS results with satellite-derived~~based~~ products and show that organized patterns in flow and topography emerge in the NEGIS~~ ice stream~~ when the surface velocity exceeds approximately 55 m a^{-1} and are related to bedrock topography.

1 Introduction

The discharge from Greenland's marine terminating outlet glaciers has increased over the last decades and contributed to the increasing mass loss from the Greenland ~~ice ~~Ice ~~sheet ~~Sheet (Mouginot et al., 2019; Mankoff et al. 2019; Imbie Team, 2019). During the same period, many outlet glaciers have accelerated and thinned in response to changes in atmospheric and oceanic forcings, thereby adding to the dynamic mass loss (Bevis et al. 2019; Khan et al., 2015). Further dynamic thinning and acceleration in ice flow at marine outlet glaciers can potentially propagate inland, and activate the vast high-elevation and slow moving interior part of the ice sheet, thereby leading to additional mass loss (Mouginot et al., 2019).

Fast flowing ice streams drain a significant fraction of the ice from the Greenland Ice Sheet into marine outlet glaciers and they thereby connect the interior parts of the ice sheet with the margins. The fast flow involves basal sliding and friction at the bed and along the shear margins, but the understanding of the mechanisms controlling ice stream dynamics and their connection to the surrounding slow-moving ice is incomplete (Minchew et al., 2019; Minchew et al., 2018; Stearns and van der Veen, 2018, Gillet-Chaulet et al. 2016). In the interior, in situ observations of surface movement are sparse and limited to a few locations (e.g. Hvidberg et al. 1997; Hvidberg et al. 2003), and satellite-derivedbased observations of surface velocity and elevation change are limited by their temporal and spatial resolution and the lack of validation data (Joughin et al., 2017). A small surface thickening is observed since 1995 from satellite altimetry in the interior, but it is not clear whether it is due to increased precipitation or ice dynamical changes (Mottram et al. 2019). As a result, there is a significant uncertainty in the projections of the future response of the interior areas of the Greenland Ice Sheet to changes at the marine outlet glaciers (Imbie Team, 2019; IPCC, 2019).

The North-East Greenland Ice Stream (NEGIS) drains a basin in northeast Greenland with an area of about 16% of the total area of the Greenland ice Ice sheet Sheet into three main marine outlet glaciers, Nioghalvfjerdsfjorden glacier (NG), Zachariae Isstrøm (ZI), and Storstrømmen Glacier (SG) (Fig. 1). NEGIS extends around 600 km upstream of its outlet glaciers to its onset near the ice divide in the interior of northern Greenland. The inferred mass loss from NEGIS has increased since after 2003 (Mouginot et al. 2019). This is mainly due to a rapid retreat of ZI since it lost its floating tongue in 2003 and a slow retreat of NG (Khan et al. 2014; Mouginot et al. 2015), while SG has slowed down after its surge around 1980 (Mouginot et al. 2018). If the marginal loss continues and induces dynamical thinning and acceleration upstream along NEGIS, it could potentially activate the interior parts of NEGIS (Khan et al., 2014; Choi et al. 2017). The onset of NEGIS in the interior may be related to the geothermal heat flux and subglacial drainage system in the area (Karlsson and Dahl-Jensen, 2015), but the sensitivity of the system to the ongoing marginal mass loss is not well known.

Here, we present results from a geodetic surface program to characterize surface topography and ice flow of an interior section of NEGIS in an area near its onset in North Central Greenland, and to assess remote sensing products from this interior area of the Greenland ice Ice sheetSheet. The area is located approximately 150 km from the ice stream onset and centered around a reference stake (75°38' N, 35°58' W) located 300 m fromnear the East Greenland Ice-core Project (EastGRIP) deep drilling site (75°38' N, 35°60' W, 2700 meters above sea level). We compare our GPS derived heights and surface velocities with the ArcticDEM height elevation model (Porter et al. 2018), as well as with 165 published and experimental remote sensing velocity products from the NASA MEaSUREs program, the ESA Climate Change Initiative, the PROMICE project, and three experimental products based on data from the ESA Sentinel-1, the DLR TerraSAR-X, and USGS Landsat satellites, in order to validate and assess these products (thesee complete list and references are given in section 4 below). We use the GPS derived horizontal surface velocities and strain rates in combination with the remote sensing velocity products to characterize the ice stream flow, shear margins and structure of NEGIS near its onset.

2 GPS data and methods

2.1 GPS stake network

The surface program includes a repeated in situ survey using the Global Positioning System (GPS) with a strain net consisting of 63 stakes. Observations cover the years 2015-2019. The stake network was established in 2015 with 16 stakes, including a central reference stake (75°38' N, 35°58' W) located 300 m from~~ near~~ the EastGRIP deep drilling site~~ (75°38' N, 35°60' W, 2700 masl)~~, and gradually expanded in 2016, 2017 and 2018 to include 63 stakes (Fig. 2). The growing network of stakes were measured by GPS every year from 2015 to 2019 and supplemented with additional temporary stakes that were measured only once. The layout of the stakes was designed to provide 1) transects of flow velocities along and transverse to the flow, and 2) longitudinal and transverse strain rates in the center of the fast flow and at both shear margins. To fulfill these requirements, the stake network contains sets of stakes placed in a diamond shape centered around the mid-point of NEGIS and at both shear margins. The stake network extends 35 km along NEGIS and 40 km across NEGIS, thereby covering the entire 25 km width of NEGIS and extending across both shear margins into the slower moving regions outside the ice stream. The purpose of the additional stakes added in 2018 was to obtain detailed information of strain rates across a topographic surface undulation northwest of NEGIS~~the EastGRIP site~~ (a 20–30 km dark/bright pattern perpendicular to NEGIS, Fig. 2a). All stake observations are included in this analysis.

The GPS observations were carried out with a Leica GX1230 GPS receiver with data acquisition lasting minimum 1 hour, and typically 2-4 hours. The GPS antenna was mounted on the top of each stake, and the height above the surface was measured manually. The stakes were 3.5 m long aluminum stakes, which~~; they~~ were drilled approximately 2 m below the surface and extended when needed due to a continuous snow accumulation in the area (approximately 0.3 m of snow equivalent per year; Vallelonga et al. 2014). All stakes established in 2015, 2016 and 2017 were extended during the observational period when the antenna heights decreased below 1 m above the surface. A few stakes were moved and/or replaced due to camp activities. The GPS observations were post-field processed using the open source software package ESA/UPC GNSS-lab tool (gLAB) (Sanz Subirana et al. 2013; Ibáñez et al. 2018). We use~~d~~ the Center for Orbit Determination in Europe (CODE) final~~the International GNSS Service (IGS) combined~~ orbit/clock product, which includes Earth rotation parameters.~~ we applied ionospheric corrections, we~~ We took the antenna phase center offset and variation into account~~, and~~. Receiver clock parameters are modelled, and the atmosphere delay parameters are modelled using the CODE maps for the ionosphere and ESA's Niell Mapping function with Simple Nominal for the troposphere. We applied solid Earth tidal corrections using the IERS Convention's degree 2 tides displacement model (Sanz Subirana et al. 2013). Ocean tidal correction is not implemented in the gLAB processing tool, and for our interior site the associated error is estimated to be within 1 cm. The coordinates are computed in the IGS14 frame. ~~we~~ We use~~d~~ the software in static mode~~.~~ and developed ~~An~~ an automated protocol~~ was developed~~ in order to perform a systematic Precise Point Positioning (PPP) processing of the stake observations. The PPP approach can introduce systematic errors if the stake is moving (King, 2004). To optimize our processing protocol and evaluate timing estimates and position uncertainties, we observed the central reference stake at the EastGRIP site (red dot in Fig. 2) over extended periods each season and compared separate 1-hour static, 24-hour static, and kinematic solutions. We found that the 24-h static solution performed better than the average position of a 24-hour kinematic solution. With a maximum observed surface speed of approximately 60 m a^{-1}, the uncertainty related to the static solution is estimated to be < 2 cm. We estimate the combined uncertainty of our GPS positions to be within 3 cm. We process the stake observations from each year, including multiple observations of some of the stakes within the annual field seasons.

The gLAB processing protocol was assessed by comparing processing results from two one-hour observations with PPP processing results from the GIPSY-OASIS version 6.4 software developed at the Jet Propulsion Laboratory (JPL). We use JPL final orbit products, which include satellite orbits, satellite clock parameters and Earth orientation parameters. The orbit products take the satellite antenna phase center offsets into account. Receiver clock parameters are modeled, and the atmospheric delay parameters are modeled using the Vienna Mapping Function 1 with VMF1 grid nominal (http://vmf.geo.tuwien.ac.at/) (Kouba, ~~2007~~2008; Boehm et al, 2006). Corrections are applied to remove the solid Earth tide and ocean tidal loading. The amplitudes and phases of the main ocean tidal loading terms are calculated using the Automatic Loading Provider (http://www.oso.chalmers.se/~loading) (Scherneck and Bos, 2002) applied to the FES2014 ocean tide model including correction for center of mass motion of the Earth due to the ocean tides. The site coordinates are computed in the IGS14 frame (Altamimi et al, 2016). All GIPSY-OASIS processing results were within ≤ 1.7 cm of the gLAB processing results (~~see~~ Table 1)~~. We note this value as our processing uncertainty.~~ and within our estimated uncertainty of 3 cm.

2.2 GPS derived velocities and surface elevations

To derive the horizontal surface velocity, a linear fit was performed to the observed Northing and Easting positions, respectively (projected to the National Snow and Ice Data Center (NSIDC) Sea Ice Polar Stereographic North and referenced to WGS84 horizontal datum (EPSG:3413)) assuming a constant displacement rate. A ~~possible~~ small tilt of the stake can lead to uncertainties in the horizontal ~~position~~velocity. We take this into account by including an unknown horizontal shift in the position of stakes that were vertically extended, and we neglect any other changes in the tilt. For each stake, the shift was determined independently from the other stakes, and the linear fit and the shift were determined simultaneously. The estimated shifts are in the range 0.05 m to 0.2 m, and often exceeds 0.10 m. The surface velocity was calculated by assuming that the flow is along the surface, thereby neglecting vertical movement. We estimate the uncertainty of the derived velocities due to the combined uncertainty of the GPS observations and the method to be in the order of 10^{-2} m a^{-1}. As a horizontal reference position of the stakes, we use the estimated horizontal position of the stakes on 2017-01-01, assuming a constant horizontal displacement of each stake over the observational period. We select a common reference for the network in order to consistently derive horizontal strain rates and assess surface elevations, but the reference date is not an accurate timestamp due to the different initial dates of the stakes.

We also estimate a mean GPS derived surface elevation of the stakes to be used below for the assessment of satellite based observations. In the interior areas of the Greenland ~~ice~~ Ice ~~sheet~~Sheet, climate driven variations in snow accumulation and firn compaction lead to seasonal and interannual variations of the surface elevation that are not resolved by our annual GPS observations. We estimate the mean GPS derived surface elevation as the mean of the individual observations at each stake, neglecting trends over the observational period due changes in snow accumulation, firn processes or ice dynamical changes.
The resulting horizontal stake velocities are shown in Figure~~.~~ 2, and the reference positions and horizontal velocities are listed in supplementary Table S1. The GPS derived surface elevations and the magnitudes of the horizontal stake velocities, are shown along three transects across NEGIS in Figure 3~~(see Fig. 3)~~ and one transect along NEGIS in Figure 4~~(see Fig. 4)~~. The stake velocities show that the surface speed is relatively constant at approximately 56.6 m a^{-1} along the centerline of NEGIS, and is above 55 m a^{-1} in central flow band wider than ~~a >~~10 km~~ wide central flow band~~. The GPS derived surface elevations reveal 20 m~~eter~~ deep topographic troughs at the shear margins. The direction of the fast flow at the center line is 33.5° from North.

2.3 GPS derived strain rates

After having derived horizontal surface velocities, we calculate horizontal strain rates, which are essential in understanding the ice flow pattern and internal stratigraphy of the ice stream and its surroundings. We calculate the horizontal principal strain rates in 32 different triangular sections within the GPS strain net. Each triangle is defined by a combination of three GPS stakes and assumes a linear velocity field within the triangle, i.e. constant strain rates within the triangles (~~see~~ Fig. 5). The principal strain rates are generally in the order of 10^{-4} a^{-1} in a wider than ~~>~~10 km~~ wide~~ central flow band along NEGIS, as well as in the slow moving areas outside NEGIS. In the two shear margins, horizontal principal strain rates increase by an order of magnitude and reach a maximum in the northern shear margin of $3.8 \cdot 10^{-3}$ a^{-1} (horizontal extension) and $-3.6 \cdot 10^{-3}$ a^{-1} (horizontal compression), and in the southern shear margin of $3.6 \cdot 10^{-3}$ a^{-1} (extension) and $-4.3 \cdot 10^{-3}$ a^{-1} (compression). In both shear margins, the principal strain rates are orientated at~~in~~ an angle of approximately ±35° relative to the direction of the flow, due to a combination of longitudinal extension, transverse compression and a high shear strain rate along the shear margins. The principal strain rates are slightly higher in the triangles north of the central flow line of NEGIS than in those south of the central flow line, probably because the northern shear margin is wider than the southern shear margin and not captured as precisely by the GPS strain net as the southern shear margin. We estimate the uncertainty of the strain rates averaged over the triangles (>2 km) to be in the order of 10^{-5} a^{-1}.
Along a transect across NEGIS, we calculate the horizontal strain rate tensor along the direction of the flow at three stakes. The three stakes are located in the northern shear margin, in the center (EastGRIP site), and in the southern shear margin, respectively (Fig. 5). The strain rates along the direction of the flow are calculated as the mean of the rotated strain rate tensors in the four adjacent triangles, and they are ±2 km horizontal averages, corresponding to the dimensions of the adjacent triangles. The normal strain rate components along the direction of the flow at these three stakes are plotted in Figure~~.~~ 3b. At

the central flow line at the EastGRIP site, the normal strain rates are (0.9±0.2)·10^{-4} a^{-1} in the longitudinal (along flow) direction, and (−0.9±0.5)·10^{-4} a^{-1} in the transverse direction. The ± 2km-average longitudinal and transverse strain rates relative to the local flow direction in the northern shear margin are (0.8±1.9)·10^{-3} a^{-1} and (−0.8±0.4)·10^{-3} a^{-1}, respectively. The horizontal shear strain rate is (−2.1±0.9)·10^{-3} a^{-1}. The ±2 km-average longitudinal and transverse strain rates relative to the local flow direction in the southern shear margin are (0.8±1.6)·10^{-3} a^{-1} and (−1.3±0.5)·10^{-3} a^{-1}, respectively, and the horizontal shear strain rate is (2.6±0.8)·10^{-3} a^{-1}. The resolution of the GPS strain net is limited by the position of the stakes and may not capture the peak strain rates at the shear margins, but the sharp transition in the southern shear margin stand out in the relative velocity pattern in Supplementary Figure~~.~~ S1 and in the strain rates along the transect across NEGIS (Fig. 3b).

~~4~~ 3 ~~Comparison with satellite observations~~Data products from satellites

~~4~~3.1 ~~Comparison with a digital elevation model observed from space~~Satellite-derived digital elevation model

The GPS derived surface elevations are used to validate the accuracy of the ArcticDEM release 7. The ArcticDEM is a digital elevation model (DEM) based on stereo auto-correlation techniques on visual imagery from Worldview satellites (Porter et al., 2018). The resolution of the ArcticDEM is 2m with a bias of less than 5m (Noh and Howat, 2015). The timestamp of the ArcticDEM in the EastGRIP area is 2017 (estimated), and the vertical accuracy has not been verified (Porter et al., 2018), thus overlapped by the GPS observation period. ~~We compare GPS derived surface elevations with the surface elevation sampled from the ArcticDEM at the stake positions (WGS84 ellipsoidal heights) and find an agreement within ±1m, except for one stake with a deviation of >1.5 m (Supplementary Fig. S2 and S3). Minor differences between the two datasets could be due to variable snow accumulation through the years, leading to seasonal and interannual variability in surface elevation, which is captured differently by the two datasets due to their different timestamps. The outlier is located in the exceptionally deep and narrow trough in the southern shear margin (Fig 3a). Local topography effects at these stakes could possibly be due to interpolation or shadow effects in the Arctic DEM (Porter et al., 2018). The mean difference between the 63 GPS derived surface elevations and the ArcticDEM at the location of the GPS stakes is 0.48 m with a standard deviation of 0.53 m, confirming the low uncertainty of the ArcticDEM (Noh and Howat, 2015; Porter et al., 2018).~~

~~4~~3.2 ~~Comparison with surface velocity products observed from space~~Satellite-derived surface velocity products

The GPS derived surface velocities are used to validate and assess the accuracy of several available ice velocity products derived from satellite data from the interior of the Greenland ~~ice~~ Ice ~~sheet~~Sheet. The ice velocity can be derived from space using data from synthetic aperture radar (SAR) or optical sensors. Optical feature tracking can provide velocities in very high resolution from coherent pairs of visual images. In the interior of the Greenland ~~ice~~ Ice ~~sheet~~Sheet, the surface is mostly featureless and SAR processing methods between pairs of SAR images are useful to derive surface velocities, either based on speckle tracking or on phase displacements from interferometric synthetic aperture radar (InSAR).

We include several experimental ice velocity products in our assessment, as well as several one-year and multi-year products constructed from various remote sensing sources and methods. For each type of velocity product, we have also calculated a long-term average of all the velocity maps, and included this in our assessment. In total, we include 165 velocity products from the following sources:

1) NASA MEaSUREs Multi-year Greenland Ice Sheet velocity map v1, 1995-2015 (Joughin et al., 2017) (MEaSUREs multi-year v1). This map was derived from InSAR, SAR, and Landsat 8 optical imagery data using a combination of speckle-tracking, InSAR and optical feature tracking methods, supplemented with balance velocities near the ice divides where the flow speeds are <5 m a^{-1}. The data are provided with a resolution of 250 m. In the interior of the ice sheet, the estimated errors of this product are up to ~2 m a^{-1}, and reported to be <1 m a^{-1} in areas where InSAR is used.

2) NASA MEaSUREs Greenland Ice Sheet winter velocity maps (September-May) from InSAR data v2, 2000-2018 (Joughin et al., 2010, 2018) (MEaSUREs InSAR v2). These maps was derived entirely from data obtained by CSA RADARSAT-1, JAXA ALOS, and DLR TerraSAR-X/TanDEM-X (TSX/TDX) satellites, as well as from ESAs C-band SAR data from Copernicus Sentinel-1A/B. The maps were produced using an integrated set of SAR, speckle-tracking and interferometric algorithms (Joughin, 2002). The data are provided with a resolution of 200 m and the error is estimated to be <10 m a^{-1}.

3) NASA MEaSUREs Greenland Annual and Quaterly Ice Sheet velocity maps from SAR and Landsat v1, 2015-2018 (Joughin et al., 2018) (MEaSURE SAR&Landsat v1). These maps are derived from SAR data obtained by DLR TerraSAR-X/TanDEM-X (TSX/TDX) and ESA Copernicus Sentinel-1A/B satellites, and from the USGS Landsat 8 optical imagery using a combination of speckle-tracking, InSAR and optical feature tracking methods (Joughin et al. 2018). The resolution of the data are 200 m.

4) ESA Climate Change Initiative (ESA CCI) Greenland Ice Sheet annual velocity maps by ENVEO, 2014-2018 from SAR (ESA Greenland Ice Sheet CCI project team, 2018). These maps are derived from ESA Copernicus Sentinel-1A/B SAR data using feature tracking techniques. The resolution is 500m, and the estimated error is ~15 m a^{-1} (Nagler et al., 2015).

5) PROMICE Greenland velocity maps, 2016-2019 from SAR (Solgaard and Kusk, 2019; available from www.promice.dk). These products are derived from ESA Copernicus Sentinel-1A/B SAR data using offset tracking (~~[~~Strozzi et al., 2002~~]~~) by employing the operational interferometric post processing chain (IPP) (Kusk et al., 2018; Dall et al., 2015). Each map is a mosaic consisting of both 12-day and 6-day pairs within two Sentinel 1A cycles, and thus the temporal resolution of the product is 24 days. A new map is available every 12 days. The spatial resolution is 500 m, and the estimated error is 10-30 m a^{-1}.

6) DTU-Space experimental Sentinel-1A/B ~~(S-1)~~ Greenland ~~ice~~ Ice ~~sheet~~ Sheet velocity product, from InSAR (DTU-Space-S1). This product is derived from SAR data acquired by ESA Copernicus Sentinel-1A/B satellites in the period from 2019-01-01 to 2019-01-18 from two ascending and three descending tracks. Eight 6-day pairs and five 12-day pairs were processed using the in-house-developed Interferometric Post Processing chain (IPP) (Kusk et al., 2018). The spatial resolution is 50 m, and the estimated errors are <1 m a^{-1} (Andersen et al., 2020).~~Interferograms were co-registered using the Tandem-X 90 m DEM and a multi-year average of the PROMICE 2016-2019 offset-tracking velocity maps (see above). The relative velocity field from each unwrapped interferogram was calibrated to absolute values using slow-moving (<0.05 m a^{-1}) ground control~~

points extracted from the same velocity map used for coregistration, and 3D velocities were generated assuming surface parallel flow.

7) AWI experimental TerraSAR-X (TSX) Greenland velocity product, from InSAR (AWI-TSX). The velocity field was derived from SAR interferometry obtained by DLR TSX by combining data from ascending and descending satellite orbits following well-established methods (e.g. Joughin et al., 1998). Three interferograms were formed from descending satellite data acquired between 2016-09-07 and 2016-10-01 and another three from ascending satellite data acquired between 2017-10-24 and 2018-01-03. All interferograms have a temporal baseline of 11 days with perpendicular baselines varying between 25 and 180 m. Due to the latter a certain topography induced phase difference is present in the interferograms, which was removed with the help of the global DLR TanDEM-X DEM with a 30 m grid resolution. The topography corrected interferograms were unwrapped using GAMMA's minimum cost flow algorithm (Werner et al., 2002) and combined to 3D velocity maps assuming surface parallel ice flow. In order to set the relative velocity estimates to absolute values seed points where extracted from the MEaSUREs multi year v1 dataset, and adjacent velocity fields where patched together using the average value in their overlapping areas. The final product was gridded to 30 m spatial resolution. The AWI-TSX product is developed for this study.

8) MEaSURE's experimental Inter-Mission Time Series of Land Ice Velocity and Elevation (ITS_LIVE) annual velocity product version Beta V0 (Gardner et al., 2019) (MEaSUREs ITS_LIVE). Surface velocities are derived from image pairs of USGS Landsat 4, 5, 7, and 8 optical imagery using the auto-RIFT feature tracking processing chain described in Gardner et al. (2018). Here we derived a multi-year velocity product from 1985 to 2018, averaged from the annual products. In our observed area, the data is mainly derived from Landsat 8, and we therefore also derive an average of the annual product from 2013 to 2018, covered by the Landsat 8 imagery. The final product was gridded to 120 m spatial resolution. The images suffers from x- and y- geolocation errors of 15 m, and to correct for these errors the velocity components are tied to a stable surface, either to zero at rock surfaces in margin areas or to the median reference velocity in slow-moving areas. In interior Greenland, the MEaSUREs Greenland Annual Ice Sheet Velocity Mosaic from SAR and Landsat version 1 velocity product is used as the reference velocity (Joughin et al., 2010). For the assessment here, we derived a multi-year velocity product from 1985 to 2018, averaged from the annual products. In our observed area, the data is mainly derived from Landsat 8, and we therefore also derived an additional 6-year average of the annual product from 2013 to 2018, covered by the Landsat 8 imagery. These two products were included in the assessment.

4 Comparison between GPS and satellite observations

4.1 Comparison between GPS data and a satellite-derived digital elevation model

We compare GPS derived surface elevations with the surface elevation sampled from the ArcticDEM release 7 at the stake positions (WGS84 ellipsoidal heights) and find an agreement within ±1m, except for one stake with a deviation of >1.5 m (Supplementary Figs. S2 and S3). Minor differences between the two datasets could be due to variable snow accumulation through the years, leading to seasonal and interannual variability in surface elevation, which is captured differently by the two datasets due to their different timestamps. The outlier is located in the exceptionally deep and narrow trough in the southern shear margin (Fig 3a). Local topography effects at these stakes could possibly be due to interpolation or shadow effects in the Arctic DEM (Porter et al., 2018). The difference between the 63 GPS derived surface elevations and the ArcticDEM at the location of the GPS stakes is 0.48 m (mean) and 0.47 m (median) with a standard deviation of 0.53 m, confirming the low uncertainty of the ArcticDEM (Noh and Howat, 2015; Porter et al., 2018).

4.2 Comparison between GPS data and surface velocity products derived from satellite data

The assessment consists of an inter-comparison between the GPS derived velocities of the stakes from the period 2015-2019 and the interpolated surface velocity at the location of the stakes from the satellite-derived~~based~~ velocity products. For each velocity product, we determine the accuracy (the bias) and precision (the standard deviation, i.e. the root mean square difference (RMS) after removing the bias), between the GPS derived velocities and the satellite-derived velocities at the location of the stakes. In addition to the direct inter-comparison between the GPS derived velocities and the satellite-derived~~based~~ velocities, we also investigate the variability of the satellite-derived~~based~~ velocity products. In order to do so, we perform a spatial smoothing of the satellite-derived~~based~~ velocity product with a running mean filter with a smoothing length, and we then vary the smoothing length in order to determine the optimum smoothing length (σ) that minimizes the standard deviation (RMS) between the GPS observations and the velocity product. The results of the inter-comparison for the top ten products (sorted according to the standard deviation) are listed in Table 2 (with a complete overview of the results from all products in Supplementary Table S2), and it is illustrated in Figure~~.~~ 6.

It is important to note that the different time stamps and temporal coverage Δt of the observations are not taken into account in the inter-comparison. In satellite-derived~~based~~ velocity products with longer temporal coverage, possible temporal variability and/or noise are smoothed, and there is a clear relationship between increasing temporal coverage and decreasing bias, standard deviation and optimum smoothing length. Similarly, spatial smoothing can remove noise. The improvement of the products with the temporal coverage Δt is significant, with the bias decreasing approximately linearly with $\sqrt{\Delta t}$, as illustrated in Figure~~.~~ 6. Some long-term products were calculated as averages of short-term products, i.e. based on more observations, which would also help reduce the temporal variability and noise of these products compared to short-term products. The bias of all the 165 products are in the range ~0.3 – 40 m a^{-1}, with a standard deviation in the range ~0.4 – 22 m a^{-1}. The velocity products already include some smoothing as part of their production, but additional ~~Smoothing~~ smoothing both temporally or spatially, for most products, reduced the standard deviation. After applying optimum spatial smoothing, the standard deviation is reduced to a range of ~0.4 – 10 m a^{-1}. The optimum smoothing length σ is typically in the order of 500-3000m.

As part of the assessment, we use the whole set of satellite-derived surface velocity products to trace flow lines along NEGIS. We use a starting point at the central reference stake near the EastGRIP site, which is located in the center of our observed area in a relatively narrow section of the NEGIS ice stream. We trace the flow lines upstream into the slower moving areas where flow converges into NEGIS and downstream into faster flow where the ice stream widens (Fig. 7). The flow lines are gradually displaced depending on their bias and fluctuate depending on their standard deviation.

5 Discussion

5.1 Assessment of surface velocity products ~~from space~~derived from satellite data

In the interior regions of the Greenland ~~ice~~ Ice ~~sheet~~Sheet, validation of satellite derived ice velocity and surface elevation products is generally limited due to lack of in-situ data. Our GPS stake network provides a unique dataset for validation in the interior accumulation area of the ice stream, and it represents a range of velocities and velocity gradients over one order of magnitude in the NEGIS ice stream, the shear margins and the surrounding slow moving areas. However, the assessment is restricted due to the limited spatial extent of the GPS data, and our conclusions may not apply to margin areas with very fast flow, seasonal variability or high surface slopes.

In our comparison, the DTU-Space-S1 experimental product stands out among all the investigated products with its short temporal coverage (~10-20 days), low bias of 0.35 m a^{-1} and the low standard deviation of 0.55 m a^{-1}, which can be reduced to 0.53 m a^{-1} after optimum smoothing of 354 m. The AWI-TSX experimental product stands out because of its minimum standard deviation of 0.39 m a^{-1} of all the investigated products, ~~and~~ its high spatial resolution, which results in a very low optimum smoothing length of 10 m, i.e. no further smoothing is needed to reduce the noise, and ~~. T~~the bias of the AWI-TSX product is 0.51 m a^{-1}, ~~and~~ also among the lowest of the investigated products. Both these products are based entirely on InSAR processing methods.

~~The~~ MEaSUREs widely used multi-year velocity product ~~from MEaSURE~~, the MEaSUREs multi-year v1 product (Joughin et al., 2017), has a bias of 0.77 m a^{-1} and a standard deviation of 0.50 m a^{-1}. Since this product is already a 20-year average, the optimum smoothing length is only 200 m and only slightly reduces the standard deviation to 0.48 m a^{-1}. It is notable, that the bias of this product is similar to several other MEaSUREs products with shorter temporal coverage, while the standard deviation of this product is smaller than the other MEaSUREs products. If the interior of the ice sheet changes slowly over time, the differences between the temporal stamp of the GPS observations and of the multi-year velocity product covering 1995-2015 may become important. However, MEaSUREs winter velocity map from 2008-2009, the MEaSUREs InSAR v2 product, performed very similar to the MEaSUREs multi-year v1 product, with a bias of 0.89 m a^{-1}, standard deviation of 0.46 m a^{-1}, and an optimum smoothing length of 51 m. The winter velocity product from 2008-2009 is based on InSAR and stands out with its low standard deviation and a relative short temporal coverage of nine months. The similar agreement between these products and the GPS derived velocities suggest that the velocity in the interior part of NEGIS has not changed significantly in the last decade.

The five products with a minimum bias are the MEaSUREs ITS_LIVE 6-year average product with a bias of 0.31 m a^{-1}, the MEaSUREs combined SAR&Landsat v1 1-year product for 2015 with a bias of 0.33 m a^{-1}, the DTU-Space-S1 18-day product from 2019 with a bias of 0.35 m a^{-1}, the ESA CCI annual velocity product from 2015-2016 with a bias of 0.43 m a^{-1}, and the 24-days PROMICE product from 2018-02 with a bias of 0.46 m a^{-1}. Of these, the DTU-Space-S1 product stands out~~ with its short temporal coverage, low standard deviation and low optimal smoothing length~~ as mentioned above. MEaSUREs ITS_LIVE product stands out with its long temporal coverage, low standard deviation, very low optimal smoothing length, and because it is the only product in our study entirely based on optical feature tracking. The other products have a time stamp that overlap with the first one to two years of the GPS observation period, but their standard deviations are much higher due to the SAR processing techniques. The MEaSUREs combined SAR&Landsat v1 product has a standard deviation of 1.85 m a^{-1}, which reduces to 1.65 m a^{-1} after optimum smoothing over 1224 m. The ESA CCI product performs very similar with a standard deviation of 1.94 m a^{-1}, which reduces to 1.11 m a^{-1} after optimum smoothing length over 1185 m. The PROMICE product with its very high temporal resolution of 24 days has a standard deviation of 5.39 m a^{-1}, which reduces to 2.6 m a^{-1} after optimum smoothing length over 2264 m.

Among the top five products with lowest standard deviation, three are entirely based on InSAR (DTU-Space-S1 from 2019; AWI-TSX from 2016-2017; MEaSUREs InSAR v2 from 2008-2009), and two are combined products averaged over a multi-year period (MEaSUREs multi-year product v1, 1995-2015; MEaSUREs multi-year SAR&Landsat v1, 2014-2018). Overall, the assessments show that for interior velocity estimates, the InSAR based products stand out with higher resolution in time and space and with lower errors. SAR speckle tracking~~based~~ products (ESA CCI, PROMICE and MEaSUREs) can obtain comparable accuracy and low standard deviation, if they are averaged over time (multi-year averages) and smoothed spatially. The optical product (MEaSUREs ITS_LIVE) can obtain a ~~comparable~~ comparably high accuracy when averaged over long time intervals (several years~~decades~~), but the standard deviation is slightly higher than the radar based products.

5.2 Inferred flowlines from satellite-derived products

Knowing the accurate flowlines of an ice sheet is useful for many applications, such as defining the outlines of drainage basins or to identify the source area for ice flowing through a specific survey site. For studies related to the internal stratigraphy and ice properties, e.g. in ice cores or radar profiles, it is essential to know the upstream flow path in order to infer the deformation history of the internal layers. However, minor uncertainties and bias in satellite-derived velocity products can severely affect flow lines traced along the velocity field, as these uncertainties can displace the flowline and propagate along the flow line (Fig. 7). The flowlines for the products with minimum bias are marked (Fig. 7), showing that flowlines can only be reliably traced if the bias is small. These products This is particularly critical when the flow is strongly convergent or divergent. We notice that the back-trajectories diverge more than the forward trajectories, and we attribute this to the higher uncertainty of the upstream lower velocities compared to downstream. As a result, it may be better to use surface slopes instead of surface velocity products to trace flow trajectories in slow moving areas.

5.~~2~~ 3 Estimated errors of ~~satellite~~ satellite-derived strain rates

Strain rates are derived from the satellite-derived~~based~~ products as derivatives of the velocity fields and have therefore higher ~~uncertainties~~errors. ~~We calculate the satellite-based strain rate tensor directly from the gridded velocity product without smoothing, and rotate according to the local flow direction in order to determine the strain rates along the flow.~~ Our assessment provides an estimate of the strain rates error depending on the resolution from the standard deviation of the velocity product. For velocity products with a standard deviation in the order of 0.5 m a^{-1}, the strain rate uncertainty is in the order of 10^{-3} a^{-1} on a 500 m grid, but it could be improved by smoothing the velocity product using the optimum smoothing length from the assessment. We compare the GPS derived strain rates with strain rates from MEaSUREs multi-year v1 velocity product in transects across the NEGIS (Fig. 3) and along NEGIS (~~fig~~Fig. 4). We calculate the satellite-derived~~based~~ strain rate tensor directly from the gridded 250 m resolution velocity product without further smoothing according to the optimum smoothing length (included in Table 2), and rotate according to the local flow direction in order to determine the strain rates along the flow. While the GPS derived strain rates are limited in resolution and do not exactly capture the maximum strain rate at the southern shear margin, they do capture the enhanced strain rates in the shear margins. The fluctuations of the satellite-derived strain rates are less than 10^{-3} a^{-1}, thus confirming our estimated uncertainty above. The satellite-derived strain rates capture the high resolution strain rate peaks of approximately $3\text{-}4 \cdot 10^{-3}$ a^{-1} in the shear margins (Fig. 3) and approximate $2 \cdot 10^{-3}$ a^{-1} along NEGIS (Fig. 4).

5.~~3~~ 4 Structure and flow of NEGIS

The assessment of satellite-derived~~based~~ velocity and height products inform of the accuracy and limitations of~~provides confidence in~~ the satellite-derived~~based~~ products in the interior regions of the Greenland ~~ice~~ Ice ~~sheets~~Sheet. In our study area the best products have a bias and precision of less than approximately 0.5 m a^{-1}, i.e. about 5% of the smallest observed GPS derived velocities of around 10 m a^{-1} in the slow-moving areas north of NEGIS. Knowing the limitations of the satellite-derived products, we are now able to combine~~Thereby, it enables us to use~~ the GPS derived velocities and strain rates ~~in combination~~ with satellite-derived~~based~~ data to characterize spatial patterns in surface structure and ice flow in the interior part of the NEGIS ice stream. We discuss here the observed patterns.

The flow and surface topography across the NEGIS ice stream reveal a distinct 25 km wide fast-flowing ice stream near the EastGRIP site, which is sharply marked at both sides in speed, strain rates and surface geometry (Fig. 3). The cross sections show a central 10 km wide section with an almost uniform speed of 55 m a^{-1}, and well-defined shear margins at both sides with a width of about 5 km separating the ice stream from the surrounding slow-moving ice (Fig. 3). The velocities are above 20 m a^{-1} on the southern side where a broad flow field is merging with NEGIS, and approximately 10 m a^{-1} on the northern side (Fig. 2 and 3). The strain rates are at a level of approximately 10^{-4} a^{-1} within the ice stream and in the surrounding slow moving areas outside the ice stream. In the shear margins, they increase ~~with~~ by an order of magnitude to a maximum value of approximately 10^{-3} a^{-1}. The ~~remarkable~~ remarkably uniform velocities and low strain rates in the fast flowing central band of NEGIS with narrow shear zones at the margins with enhanced strain rates is characteristic of ice stream flow (e.g. Minchew et al., 2018). In our study area in NEGIS, Holschuh et al. (2019) proposed that thermal~~, support a~~ softening of ~~the~~ ice is present in the shear margins, despite the relatively low strain rates ~~due to higher temperatures or ice fabric (Holschuh et al., 2019)~~. The surface topography reveals a 30-40 m deep ~~trough~~ lowering coinciding with the fast flow within NEGIS ~~and~~ with ~~an additional~~ well-defined ~~10-20 m~~ deep troughs marking the shear margins. These deep shear margin troughs form due to a combination of enhanced longitudinal stretching~~, transverse compression~~ and shear as the ice flow enters the fast flowing ice stream from both sides ~~with~~ at an angle of ~15°, accelerates and turns, and an enhanced firn densification in the shear margins due to the enhanced horizontal deformation (Riverman et al., 2019a).

The location of the shear margins cannot be clearly linked to the bedrock topography in the area (Christianson et al., 2014; Franke et al., 2020). Christianson et al. (2014) proposed that the shear margins of NEGIS are controlled by a self-stabilizing mechanism related to gradients in the subglacial hydropotential due to the surface troughs that restrict widening of the ice stream, and the internal stratigraphy suggests that the shear margins have been relatively stable during the Holocene (Keisling et al., 2014). Detailed maps of bedrock topography in the area reveal subglacial landforms proposed to be related to basal erosion due to the fast flow (Franke et al., 2020), and elongated bedforms aligned with the flow (Franke et al., 2020; Riverman et al., 2019b). These elongated bedforms are seen in the transects across NEGIS as 100-300 m undulations in bedrock topography (Fig. 3), and they appear here to be related to the location of the shear margins. The southern very well-defined shear margin trough is consistently located above a local bedrock low in the three cross sectional profiles spanning a 5 km distance along NEGIS (Fig. 3). The northern broad shear margin trough is located over a wide bedrock valley, and the shear margin trough narrows from a wide double-trough to a single trough in the three cross sectional profiles over a 5 km distance along NEGIS, as the bedrock valley over the same distance narrows (Fig. 3). Thus, our observations support that these bedforms are related to the shear margins (Franke et al., 2020; Riverman et al., 2019b), but further studies are needed to fully understand the conditions at the shear margins.

The ArcticDEM surface topography of the NEGIS ice stream shows that an organized spatial pattern of wavy undulations develops perpendicular to the NEGIS flow in the area around EastGRIP (Fig. ~~7~~8). The undulations develop within the fast flowing central flow band of NEGIS in a 25 km section along NEGIS where the surface velocity remain at a level of approximately 55 m a^{-1}. Upstream from this section, the flow accelerates over tens of km with an acceleration of approximately 10 m a^{-1} over 10 km, i.e. longitudinal strain rates of ~10^{-3} a^{-1}. The undulating patterns start forming as ice velocity exceeds a threshold velocity of approximately 55 m a^{-1}, and as the ice flows over a 200-300 m bedrock transition to a bedrock plateau of approximately 200 m elevation and widens (Franke et al., 2020), suggesting that the undulations are related to the bedrock topography (Fig. 4). The undulations in surface slope are connected to undulations in the longitudinal and transverse surface strain rates, and to some degree related to undulations in bedrock topography (Fig. 4). Similar organized undulating patterns in driving stress was previously reported in Antarctic and Greenland ice sheets in fast flowing areas (Sergienko and Hindmarsh, 2013; Sergienko et al., 2014) and related to patterns in basal stress located in areas with significant sliding. These previous studies attributed the patterns to be the result of instabilities related to subglacial water beneath a sliding glacier, and our results support that bedrock topography plays a role in relation to these undulations.

5.4 Inferring the upstream flow path from velocity products

Knowing the accurate flowlines of an ice sheet is useful for many applications, such as defining the outlines of drainage basins or to identify the source area for ice flowing through a specific survey site. For studies related to the internal stratigraphy and ice properties, e.g. in ice cores or radar profiles, it is essential to know the upstream flow path in order to infer the deformation history of the internal layers. However, minor uncertainties and bias in satellite-based velocity products can severely affect flow lines traced along the velocity field, as these uncertainties can displace the flowline and propagate along the flow line. This is particularly critical when the flow is strongly convergent or divergent. To investigate this, we use the whole set of satellite-derived surface velocity products to trace flow lines along NEGIS. We use a starting point at the EastGRIP site, located in the center of our observed area in a relatively narrow section of the NEGIS ice stream. We trace the flow lines upstream into the slower moving areas where flow converges into NEGIS and downstream into faster flow where the ice stream widens. These flow lines differ widely depending on the bias and standard deviation of the products (Fig. 8). We notice that the back trajectories diverge more than the forward trajectories, and we attribute this to the higher uncertainty of the upstream lower velocities compared to downstream. As a result, it may be better to use surface slopes instead of surface velocity products to trace flow trajectories in slow moving areas.

6 Conclusion

We have presented results from a GPS survey in 2015-2019 of a strain net consisting of 63 stakes near the EastGRIP deep drilling site in the interior northeast Greenland to map surface topography and flow of an interior section of NEGIS in an area near its onset in interior North Greenland. The GPS derived surface velocities are >55 m a^{-1} within an approximately 10 km wide central flow band, and drops abruptly at the shear margins to approximately 10 m a^{-1} and 25 m a^{-1} at the northern and southern sides, respectively. The flow enters NEGIS at an angle of approximately 15° from both sides. Strain rates are in the order of 10^{-3} a^{-1} in the shear margins with enhanced longitudinal stretching, transverse compression and shearing, and an order of magnitude smaller elsewhere. Our results suggest that the location of the shear margins is related to 100-300 m bedrock lows.

We compare our GPS derived heights and surface velocities with the ArcticDEM height model (Porter et al., 2018), as well as published and experimental remote sensing velocity products in order to validate and assess these products. We include surface velocity products from the MEaSUREs program, the ESA CCI program, the PROMICE program, and experimental data products from MEaSUREs, DTU-Space and AWI. For each product, we calculate the bias, the standard deviation relative to the GPS derived surface velocities, and the spatial smoothing that minimizes the standard deviation. Our assessments show:

- the ArcticDEM height model is accurate at the strain net poles within 0.48 m with a standard deviation of 0.53 m compared to the GPS positions, without considering the different time stamps of the observations. The uncertainty of the GPS positions is in the order of ~~10^{-2}~~ 0.01 m.
- Among the top five surface velocity products with lowest standard deviation compared to the GPS derived surface velocities, three are entirely based on InSAR (DTU-Space, 2019; AWI-TSX, 2016-2017; MEaSUREs winter velocity by InSAR v2, 2008-2009), and two are combined products averaged over a multi-year period (MEaSUREs multi-year product, 1995-2015; MEaSUREs multi-year SAR and Landsat, 2014-2018).
- SAR based surface velocity products from ESA CCI, PROMICE and MEaSUREs can obtain comparable precision compared to the GPS derived surface velocities if they are averaged over longer time periods (years) and smoothed spatially, and they generally obtain a low bias.
- The experimental optical velocity product from MEaSUREs can also obtain a comparable precision as the SAR based products if it is averaged over long periods (several years), but the bias is slightly higher.

Overall, the assessments show that for interior velocity estimates, the InSAR based products stand out with higher resolution in time and space and low errors. For all products, longer observation time improves the products in these interior areas where surface velocity has not changed significantly over the last decade.

The assessment inform of the accuracy of the satellite-derived velocities, and thereby allow us to evaluate the use of these products for investigations of flow patterns in the interior regions of the Greenland Ice Sheet. We show that satellite-derived strain rates can capture high-resolution spatial signals at the shear margins and within the fast flowing part of NEGIS, despite the high uncertainty in the order of 10^{-3} a^{-1}. We show further that the strain rate peaks along NEGIS are part of a ~~We investigate flow along the centerline of NEGIS and find that~~ regular undulating pattern~~s~~ forming in surface slope and strain rates when the surface velocity exceeds approximately 55 m a^{-1}, and we argue that the formation of these undulations appears to be related to bedrock topography. ~~Finally, we investigated the uncertainties in derived flow trajectories along NEGIS depending on the accuracy and precision of the satellite derived velocity products. We traced flow lines from our observed area, and show that the flow lines differ significantly among the assessed products depending on their bias.~~

We derived flowlines from the satellite-derived velocity products and showed that even a minor bias in these products can severely affect the path of the flowlines, in particular in slow-moving areas. We conclude that reliable flowlines can only be derived from satellite-derived velocities with a low bias of less than 1% compared to the surface speed, and that surface slopes may produce more realistic flowlines than satellite-derived velocities in slow-moving areas.

The study demonstrates that it is important to know the limitations of the satellite-derived products. We conclude that available satellite-derived products are sufficiently accurate to allow a detailed analysis of the ice flow in the interior part of NEGIS, which can contribute to understand the flow near its onset in interior North Greenland, and ultimately to improve projections of its future response to mass loss at the margins.

Author contributions: C.S.H. and A.G. designed and carried out the study. H.A.K., P.V., N.B.K. and D.D.J. contributed to the field work. S.A.K. contributed to the design of the GPS survey and the validation of the GPS processing with GIPSY-OASIS software. N.N., A.S., A.K. and J.K.A. provided remote sensing velocity products. C.S.H. and A.G. prepared the draft manuscript, and all authors provided comments and input to the manuscript.

Competing interests: The authors declare that they have no conflict of interest.

Acknowledgments: This work was supported by a Dancea grant from the Danish Environmental Protection Agency (EPA), by the PROMICE project, by the European Space Agency (ESA) Climate Change Initiative (CCI, CCI+) Greenland ~~ice~~ Ice ~~sheet~~ Sheet project (contracts No. 4000112228 and 4000126523), and by research grants from the Villum Foundation (grant No. 2361 and 16572). Logistical support was provided by the East Greenland Ice-Core Project. EastGRIP is directed and organized by the Center of Ice and Climate at the Niels Bohr Institute. It is supported by funding agencies and institutions in Denmark (A. P. Møller Foundation, University of Copenhagen), the USA (U.S. National Science Foundation, Office of Polar Programs), Germany (AlfredWegener Institute, Helmholtz Centre for Polar and Marine Research), Japan (National Institute of Polar Research and Arctic Challenge for Sustainability), Norway (University of Bergen and Bergen Research Foundation), Switzerland (Swiss National Science Foundation), France (French Polar Institute Paul-Emile Victor, Institute for Geosciences and Environmental research), and China (Chinese Academy of Sciences and Beijing Normal University). TerraSAR-X and TanDEM-X data used in the processing of surface velocities were made available through DLR proposals HYD2059 and DEM_GLAC1608. N.N. received funding from the European Union's Horizon 2020 research and innovation programme under grant agreement No. 689443 via project iCUPE (Integrative and Comprehensive Understanding on Polar Environments). The ArcticDEM was provided by the Polar Geospatial Center under NSF-OPP awards 1043681, 1559691, and 1542736. Ice velocity maps were produced as part of the Programme for Monitoring of the Greenland Ice Sheet (PROMICE) using Copernicus Sentinel-1 SAR images distributed by ESA, and were provided by the Geological Survey of Denmark and Greenland (GEUS) at http://www.promice.dk

References

Altamimi, Z., P. Rebischung, L. Metivier, and X. Collilieux: ITRF2014: A new release of the International Terrestrial Reference Frame modeling nonlinear station motions, J. Geophys. Res. Solid Earth, 121, doi:10.1002/2016JB013098, 2016.

Andersen, J. K., A. Kusk, J. P. M. Boncori, C. S. Hvidberg, A. Grinsted: Improved Ice Velocity Measurements with Sentinel-1 TOPS Interferometry. Remote Sensing, 12(12), [2014]. https://doi.org/10.3390/rs12122014, 2020.

Bevis, M., J. Wah, S. A. Khan, F. B. Madsen, A. Brown, M. Willi, E. Kendricka, P. Knudsen, J. E. Box, T. van Dam, D. J. Caccamise II, B. Johns, T. Nylen, R. Abbott, S White, J. Miner, R. Forsberg, H. Zhou, J. Wang, T. Wilson, D. Bromwiche, and O. Francis: Bedrock displacements in Greenland manifest ice mass variations, climate cycles and climate change. PNAS, doi:10.1073/pnas.1204664109, 2019.

Boehm J., B. Werl, H. Schuh: Troposphere mapping functions for GPS and very long baseline interferometry from European Centre for medium-range weather forecasts operational analysis data. J. Geophys. Res. 111, B02406, doi:10.1029/2005JB003629, 2006.

Choi, Y., Morlighem, M., Rignot, E., Mouginot, J., & Wood, M.: Modeling the response of Nioghalvfjerdsfjorden and Zachariae Isstrøm glaciers, Greenland, to ocean forcing over the next century. Geophysical Research Letters, 44, 11,071–11,079, doi.org/10.1002/2017GL075174, 2017.

Christianson, K., L. E. Peters, R. B. Alley, A. Anandakrishnan, R. W. Jacobel, K. L. Riverman, A. Muto and B. A. Keisling: Dilatant till facilitates ice-stream flow in northeast Greenland. Earth and Planetary Science Letters, 401, 57-69, https://doi.org/10.1016/j.epsl.2014.05.060, 2014.

Dall, J., Kusk, A., Nielsen, U., Merryman Boncori, J.P.: Ice Velocity Mapping Using TOPS SAR Data and Offset Tracking. In: Proceedings of 9th International Workshop Fringe 2015. ESA Publication SP-731. https://doi:10.5270/Fringe2015.91, 2015.

ESA Greenland Ice Sheet CCI project team. ESA Greenland Ice Sheet Climate Change Initiative (Greenland_Ice_Sheet_cci): Greenland Ice Velocity Map, Winter 2015-2016, v1.2. Centre for Environmental Data Analysis, *2020-02-18*. https://catalogue.ceda.ac.uk/uuid/ 302f379334e84664bd3409d08eca6565, 2018.

Franke, S., Jansen, D., Binder, T., Dörr, N., Helm, V., Paden, J., Steinhage, D. and Eisen O.: Bed topography and subglacial landforms in the onset region of the Northeast Greenland Ice Stream. Annals of Glaciology, 1–11. https://doi.org/10.1017/aog.2020.12, 2020.

Gardner, A. S., G. Moholdt, T. Scambos, M. Fahnstock, S. Ligtenberg, M. van den Broeke, and J. Nilsson: Increased West Antarctic and unchanged East Antarctic ice discharge over the last 7 years, Cryosphere, 12(2): 521–547, doi:10.5194/tc-12-521-2018, 2018.

Gardner, A. S., M. A. Fahnestock, and T. A. Scambos:, ITS_LIVE Regional Glacier and Ice Sheet Surface Velocities. Data archived at National Snow and Ice Data Center; doi:10.5067/6II6VW8LLWJ7, 2019 [2019-05-01].

Gillet-Chaulet, F., G. Durand, O. Gagliardini, C. Mosbeux, J. Mouginot, F. Rémy, and C. Ritz: Assimilation of surface velocities acquired between 1996 and 2010 to constrain the form of the basal friction law under Pine Island Glacier, Geophys. Res. Lett., 43, 10,311–10,321, doi:10.1002/2016GL069937, 2016.

Holschuh, N., Lilien, D. A., and Christianson, K.: Thermal weakening, convergent flow, and vertical heat transport in the Northeast Greenland Ice Stream shear margins. Geophysical Research Letters, 46, 8184–8193. https://doi.org/10.1029/2019GL083436, 2019.

Hvidberg, C. S., K. Keller, N. S. Gundestrup, C. C. Tscherning and R. Forsberg: Mass balance and surface movement of the Greenland Ice Sheet at Summit, Central Greenland. Geophys. Res. Letters, 24(18), 2307-2310, https://doi.org/10.1029/97GL02280, 1997.

Hvidberg, C. S., K. Keller, and N. S. Gundestrup: Mass balance and ice flow along the north-northwest ridge of the Greenland ice sheet at NorthGRIP. Annals of Glaciology, 35, 521-526, https://doi.org/10.3189/172756402781816500, 2002.

Ibáñez D., Rovira-García A., Sanz J., Juan JM., Gonzalez-Casado G., Jimenez-Baños D., López-Echazarreta C., Lapin I. The GNSS Laboratory Tool Suite (gLAB) updates: SBAS, DGNSS and Global Monitoring System. 9th ESA Workshop on Satellite Navigation Technologies (NAVITEC 2018), Noordwijk, The Netherlands. December 5 - 7, 2018. DOI: 10.1109/NAVITEC.2018.8642707, 2018.

IMBIE Team: Mass balance of the Greenland Ice Sheet from 1992 to 2018. Nature, https://doi.org/10.1038/s41586-019-1855-2, 2019.

IPCC: IPCC Special Report on the Ocean and Cryosphere in a Changing Climate. H.-O. Pörtner, D.C. Roberts, V. Masson-Delmotte, P. Zhai, M. Tignor, E. Poloczanska, K. Mintenbeck, A. Alegría, M. Nicolai, A. Okem, J. Petzold, B. Rama, N.M. Weyer (eds.). In press, 2019.

Joughin, I.R., R. Kwok and M.A. Fahnestock: Interferometric estimation of three-dimensional ice-flow using ascending and descending passes. IEEE Trans. Geosci. Remote Sens., 36(1), 25–37, doi: 10.1109/36.655315, 1998.

Joughin, I.: Ice-sheet velocity mapping: a combined interferometric and speckle-tracking approach. Annals of Glaciology, 34, 195-201, doi: 10.3189/172756402781817978, 2002.

Joughin, I., Smith, B. E., Howat, I. M., Scambos, T., and Moon, T.: Greenland flow variability from ice-sheet-wide velocity mapping, J. Glaciol., 56, 415–430, doi: 10.3189/002214310792447734, 2010.

Joughin, I., B. Smith, I. Howat, and T. Scambos: MEaSUREs Multi-year Greenland Ice Sheet Velocity Mosaic, Version 1. NASA National Snow and Ice Data Center Distributed Active Archive Center, Boulder, Colorado USA. doi: https://doi.org/10.5067/QUA5Q9SVMSJG. 2016.

Joughin, I., B. E. Smith, and I. M. Howat: A complete map of Greenland ice velocity derived from satellite data collected over 20 years. Journal of Glaciology, doi: 10.1017/jog.2017.73, 2017.

Joughin, I., Smith, B. E., and Howat, I.: Greenland Ice Mapping Project: ice flow velocity variation at sub-monthly to decadal timescales, The Cryosphere, 12, 2211–2227, https://doi.org/10.5194/tc-12-2211-2018, 2018.

Karlsson, N. B. and D. Dahl-Jensen: Response of the large-scale subglacial drainage system of Northeast Greenland to surface elevation changes. The Cryosphere, 9, 1465-1479, doi:10.5194/tc-9-1465-2015, 2015.

Keisling, B. A., K. Christianson, R. B. Alley, L. E. Peters, J. E. M. Christian, S. Anandakrishnan, K. L. Riverman, A. Muto and R. W. Jacobel: Basal conditions and ice dynamics inferred from radar-derived internal stratigraphy of the northeast Greenland ice stream. Annals of Glaciology, 55(67), 127-137, doi:10.3189/2014AoG67A090, 2014.

Khan, S. A., Kjaer, K. H., Bevis, M., Bamber, J. L., Wahr, J., Kjeldsen, K. K., Bjork, A. A., Korsgaard, N. J., Stearns, L. A., van den Broeke, M. R., Liu, L., Larsen, N. K., and Muresan, I. S.: Sustained mass loss of the northeast Greenland ice sheet triggered by regional warming. Nature Climate Change, 4(4), 292-299, doi: 10.1038/NCLIMATE2161, 2014.

Khan, S. A., A. Aschwanden, A. A. Bjørk, J. Wahr, K. K. Kjeldsen, and K. H. Kjær: Greenland ice sheet mass balance: a review. Rep. Prog. Phys. 78, doi:10.1088/0034-4885/78/4/046801, 2015.

King, M.: Rigorous GPS data-processing strategies for glaciological applications. Journal of Glaciology, 50 (171), 601-607, doi: 10.3189/172756504781829747, 2004.

Kouba, J.: Implementation and testing of the gridded Vienna Mapping Function 1 (VMF1). J. ~~Geophys. Res~~Geod. 82, 193–205, ~~2007.~~doi: 10.1007/s00190-007-0170-0, 2008.

Kusk, A., Boncori, J.P.M., Dall, J.: An automated system for ice velocity measurement from SAR. In Proceedings of the 12th European Conference on Synthetic Aperture Radar (EUSAR 2018), 929-932, VDE Verlag. Proceedings of the European Conference on Synthetic Aperture Radar, 2018.

Mankoff, K. D., W. Colgan, A. Solgaard, N. B. Karlsson, A. P. Ahlstrøm, D. van As, J. E. Box, S. A. Khan, K. K. Kjeldsen, J. Mouginot, and R. S. Fausto: Greenland Ice Sheet solid ice discharge from 1986 through 2017. Earth Syst. Sci. Data, 11, 769–786, https://doi.org/10.5194/essd-11-769-2019, 2019.

Minchew, B. M., C. R. Meyer, A. A. Robel, G. H. Gudmundsson, and M. Simons: Processes controlling the downstream evolution of ice rheology in glacier shear margins: case study on Rutford Ice Stream, West Antarctica. Journal of Glaciology (2018), 64(246) 583–594 doi: 10.1017/jog.2018.47, 2018.

Minchew, B. M., C. R. Meyer, S. S. Pegler, B. P. Lipovsky, A. W. Rempel, G. H. Gudmundsson, N. R. Iverson: Comment on 'Friction at the bed does not control fast glacier flow'. 2019. Science, 363, doi: 10.1126/science.aau6055, 2019.

Morlighem M. M., C. N. Williams, E. Rignot, L. An, J. E. Arndt, J. L. Bamber, G. Catania, N. Chauché, J. A. Dowdeswell, B. Dorschel, I. Fenty, K. Hogan, I. Howat, A. Hubbard, M. Jakobsson, T. M. Jordan, K. K. Kjeldsen, R. Millan, L. Mayer, J. Mouginot, B. P. Y. Noël, C. O'Cofaigh, S. Palmer, S. Rysgaard, H. Seroussi, M. J. Siegert, P. Slabon, F. Straneo, M. R. van den Broeke, W. Weinrebe, M. Wood, and K. B. Zinglersen: BedMachine v3: Complete bed topography and ocean bathymetry mapping of Greenland from multi-beam echo sounding combined with mass conservation, Geophys. Res. Lett., 44, doi:10.1002/2017GL074954, 2017a.

Morlighem, M. et al.: IceBridge BedMachine Greenland, Version 3. NASA National Snow and Ice Data Center Distributed Active Archive Center, Boulder, Colorado USA. doi: https://doi.org/10.5067/2CIX82HUV88Y. 2017b.

Mottram, R., S.B. Simonsen, S.H. Svendsen, V. Barletta, L.S. Sørensen, J. Wuite, T. Nagler, A. Groh, M. Horwarth, J. Rosier, A.M. Solgaard, C.S. Hvidberg and R. Forsberg: An integrated view of Greenland Ice Sheet mass changes based on models and satellite observations. Remote Sensing, 11(12), 1407 https://doi.org/10.3390/rs11121407, 2019.

Mouginot J., E. Rignot, B. Scheuchl, I. Fenty, A. Khazendar, M. Morlighem, A. Buzzi, and J. Paden: Fast retreat of Zachariae Isstrøm, northeast Greenland. Science 350:1357–1361, doi: 10.1126/science.aac7111, 2015.

Mouginot J., Bjørk A. A., Millan R., Scheuchl B., and Rignot E.: Insights on the surge behavior of Storstrømmen and L. Bistrup Brae, Northeast Greenland, over the last century. Geophys Res Lett 45:11197–11205, doi: 10.1029/2018GL079052, 2018.

Mouginot, J., E. Rignot, A. A. Bjørk, M. van den Broeke, R. Millan, M. Morlighem, B. Noël, B. Scheuchl, and M. Wood: Forty-six years of Greenland Ice Sheet mass balance from 1972 to 2018. Proceedings of the National Academy of Sciences May 2019, 116 (19) 9239-9244; DOI: 10.1073/pnas.1904242116, 2019.

Nagler, T., H. Rott, M. Hetzenecker, J. Wuite, and P. Potin: The Sentinel-1 Mission: New Opportunities for Ice Sheet Observations. Remote Sensing, 7, 9371-9389, doi:10.3390/rs70709371, 2015.

Noh, M.-J., and I. M. Howat~~. 2015.~~: Automated stereo-photogrammetric DEM generation at high latitudes: Surface extraction with TIN-based search-space minimization (SETSM) validation and demonstration over glaciated regions. GIScience & Remote Sensing 52 (2): 198–217. doi:10.1080/15481603.2015.1008621, 2015.

Porter, C., Morin, P., Howat, I., Noh, M.-J., Bates, B., Peterman, K., Keesey, S., Schlenk, M., Gardiner, J., Tomko, K., Willis, M., Kelleher, C., Cloutier, M., Husby, E., Foga, S., Nakamura, H., Platson, M., Wethington, M. Jr., Williamson, C., Bauer, G., Enos, J., Arnold, G., Kramer, W., Becker, P., Doshi, A., D'Souza, C., Cummens, P., Laurier, F., Bojesen, M.: ArcticDEM. https://doi.org/10.7910/DVN/OHHUKH, Harvard Dataverse, V1, 2018 [Date Accessed 2017-06-07].

Riverman, K. L., Alley, R. B., Anandakrishnan, S., Christianson, K., Holschuh, N. D., Medley, B., Muto, A., and Peters, L. E.: Enhanced firn densification in high-accumulation shear margins of the NE Greenland Ice Stream. Journal of Geophysical Research: Earth Surface, 124, 365–382. https://doi.org/10.1029/2017JF004604, 2019a.

Riverman, K. L., S. Anandakrishnan, R. B. Alley, N. Holschuh, C. F. Dow, A. Muto, B. R. Parizek, K. Christianson, and L. E. Peters: Wet subglacial bedforms of the NE Greenland Ice Stream shear margins. Annals of Glaciology 60(80), 91–99. https://doi.org/10.1017/aog.2019.43, 2019b.

Sanz Subirana, J., Juan Zornoza, J. M., & Hernández-Pajares, M.: GNSS Data Processing Book, Vol. I: Fundamentals and Algorithms. TM-23/1. Noordwijk: ESA Communications, 2013. ISBN: 978-92-9221-886-7.

Scherneck, H. G., and M. S. Bos: Ocean tide and atmospheric loading. In: IVS 2002 General Meeting Proceedings, Tsukuba, Japan, February 4-7, 2002.

Sergienko, O. V., and R. C. A. Hindmarsh: Regular patterns in frictional resistance of ice-stream beds seen by surface data inversion. Science, 342(6162), 1086–1089, doi:10.1126/science.1243903, 2013.

Sergienko,O. V., T. T. Creyts, and R. C. A. Hindmarsh: Similarity of organized patterns in driving and basal stresses of Antarctic and Greenland ice sheets beneath extensive areas of basal sliding, Geophys. Res. Lett., 41, doi:10.1002/2014GL059976, 2014.

Solgaard, A., and A. Kusk: Programme for monitoring of the Greenland ~~ice~~ Ice ~~sheet~~ Sheet (PROMICE): Greenland ice velocity. Geological survey of Denmark and Greenland (GEUS), doi: https://doi.org/10.22008/PROMICE/DATA/SENTINEL1ICEVELOCITY/GREENLANDICESHEET/V1.0.0, 2019.

Stearns, L. A. and C. van der Veen: Friction at the bed does not control fast glacier flow. Science 361, 273–277 (2018), doi: 10.1126/science.aat2217, 2018.

Strozzi, T., A. Luckman, T. Murray, U. Wegmuller, and C. L. Werner: Glacier motion estimation using SAR offset-tracking procedures, IEEE Trans. Geosci. Remote Sens., 40(11), 2384–2391, doi: 10.1109/TGRS.2002.805079, 2002.

Vallelonga, P., K. Christianson, R. B. Alley, S. Anandakrishnan, J. E. M. Christian, D. Dahl-Jensen, V. Gkinis, C. Holme, R. W. Jacobel, N. B. Karlsson, B. A. Keisling, S. Kipfstuhl, H. A. Kjær, M. E. L. Kristensen, A. Muto, L. E. Peters, T. Popp, K. L. Riverman, A. M. Svensson, C. Tibuleac, B. M. Vinther, Y. Weng, and M. Winstrup: Initial results from geophysical surveys and shallow coring of the Northeast Greenland Ice Stream (NEGIS). The Cryosphere, 8, 1275–1287, doi:10.5194/tc-8-1275-2014, 2014.

Werner, C., U. Wegmüller, T. Strozzi, and A. Wiesmann: Proces~~-~~sing strategies for phase unwrapping for INSAR applications, Proceedings of ~~paper presented at~~ European Conference on Synthetic Aperture Radar: EUSAR2002, ~~Verband der Elektrotech. Elektron. Informationstechnik,~~ Cologne, Germany, 4–6 June, 2002.

Comparison of results	Stake No.	ΔNE (m)	ΔH (m)
GPS (gLAB vs. GIPSY-OASIS)	Rx85 2018	0.0037	0.0039
	Rx85 2019	0.0165	0.0143
GPS (gLAB vs. CSRS-PPP)	Rx85 2018	0.0060	0.0121
	Rx85 2019	0.0018	0.0176
GPS (GIPSY-OASIS vs. CSRS-PPP)	Rx85 2018	0.0026	0.0082
	Rx85 2019	0.0167	0.0032

Table 1. Assesment of the GPS positions for two stake observations in 2018 and 2019. Top lines: assessment of the processing results, gLAB vs. GIPSY-OASIS. The processing results from the open source Canadian service CSRS-PPP software v. 1.05 is shown for comparison. ΔNE is the difference in horizontal positions, and ΔH is the difference in vertical positions.

Product	t_start	t_end	Δt (a)	bias (m)	RMS (m)	σ (m)	δ (m)
AWI-TSX	2016-09-07	2018-01-03	1.2923	0.51~~2756~~	0.39~~88398~~	10~~.01~~	30
MEaSUREs InSAR v2	2008-09-15	2009-06-16	0.7502	0.89~~0984~~	0.46~~58783~~	51~~.07~~	500
MEaSUREs Multi-year v1	1995-01-12	2015-10-31	20.7995	0.77~~67592~~	0.50~~495511~~	202~~.48~~	250
DTU-Space-S1	2019-01-01	2019-01-18	0.0465	0.35~~2026~~	0.55~~48307~~	354~~3.97~~	50
MEaSUREs SAR&Landsat v1	2014-12-01	2018-11-30	3.9973	0.55~~3502~~	0.70~~69771~~4	380~~79.91~~	500
ENVEO ESA CCI	2014-10-01	2019-04-12	4.5284	1.28~~2672~~	0.71~~3517~~	594~~3.75~~	250
PROMICE	2016-09-14	2019-06-17	2.7543	1.00~~0318~~	0.74~~38214~~	449~~8.83~~	500
MEaSUREs ITS_LIVE	2013-01-01	2018-01-01	5.9959	0.31~~06062~~	0.87~~66842~~	27~~.34~~	240
MEaSUREs ITS_LIVE	1985-01-01	2020-04-01	35.2471	0.47~~67395~~	0.88~~0819~~	381~~0.93~~	120
MEaSUREs ITS_LIVE	2018-01-01	2018-12-31	0.9966	0.65~~45198~~	0.95~~4738~~	51~~0.90~~	240

Table 2. The~~ table shows the~~ assessment results for the ten velocity products with the smallest standard deviation (RMS). The products are sorted with increasing RMS. Notice that the AWI-TSX, the DTU-Space-S1, and the MEaSUREs ITS_LIVE products are also among the ten products with the smallest bias. The bias is here the absolute value of the bias. The complete list of assessment results can be found in Supplementary Table S2.

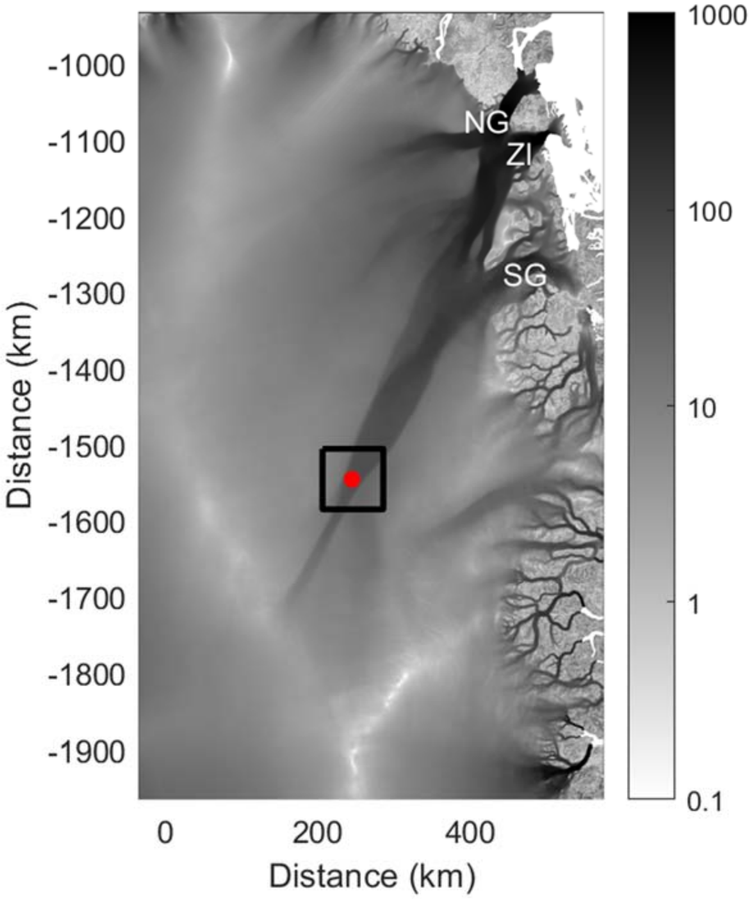

NG
ZI
SG
-1000
-1100
-1200
-1300
-1400
-1500
-1600
-1700
-1800
-1900
Distance (km)
0
200
400
Distance (km)
1000
100
10
1
0.1

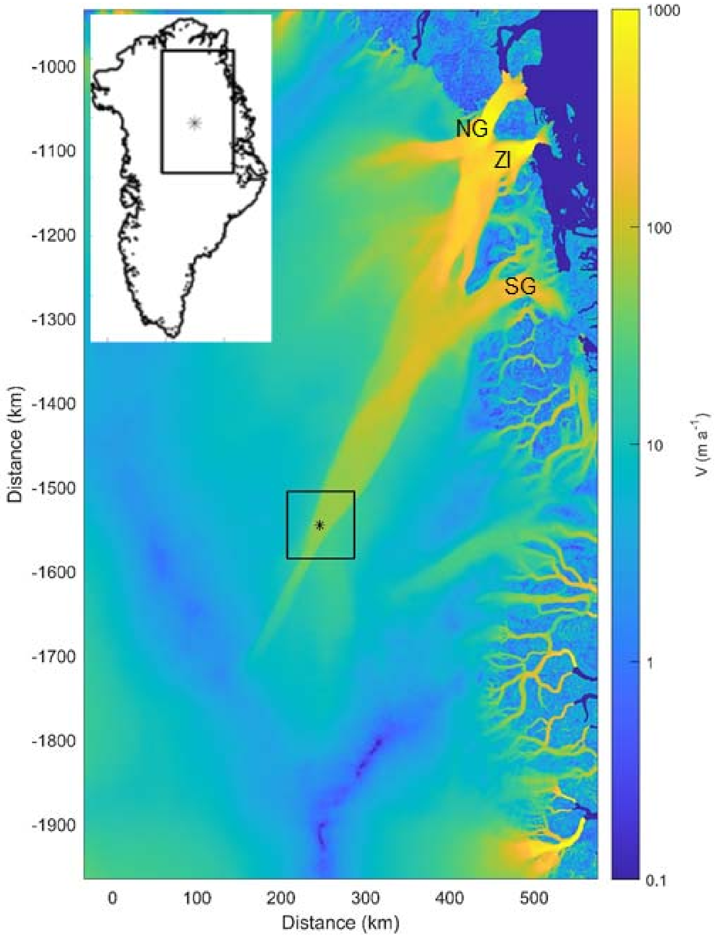

Figure 1. Map of the surface velocity in NE Greenland in m a^{-1} from MEaSUREs multi-year Greenland Ice Sheet velocity v1 product, 1995-2015 (Joughin et al., 2016, 2017), showing the NEGIS ice stream and its three main outlets, Nioghalvfjerdsfjorden glacier (NG), Zachariae Isstrøm (ZI), and Storstrømmen Glacier (SG). The black box shows the outline of the map in Fig. 2, and the ~~red~~ black star~~dot~~ indicates the EastGRIP site (75°38'N, 35°60'W). The inset map shows the location in Greenland.

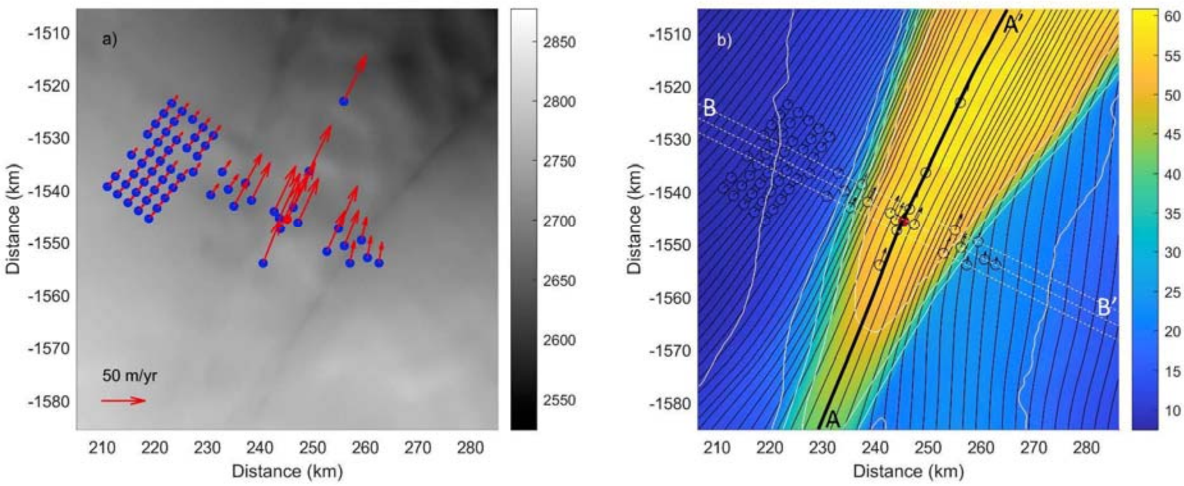

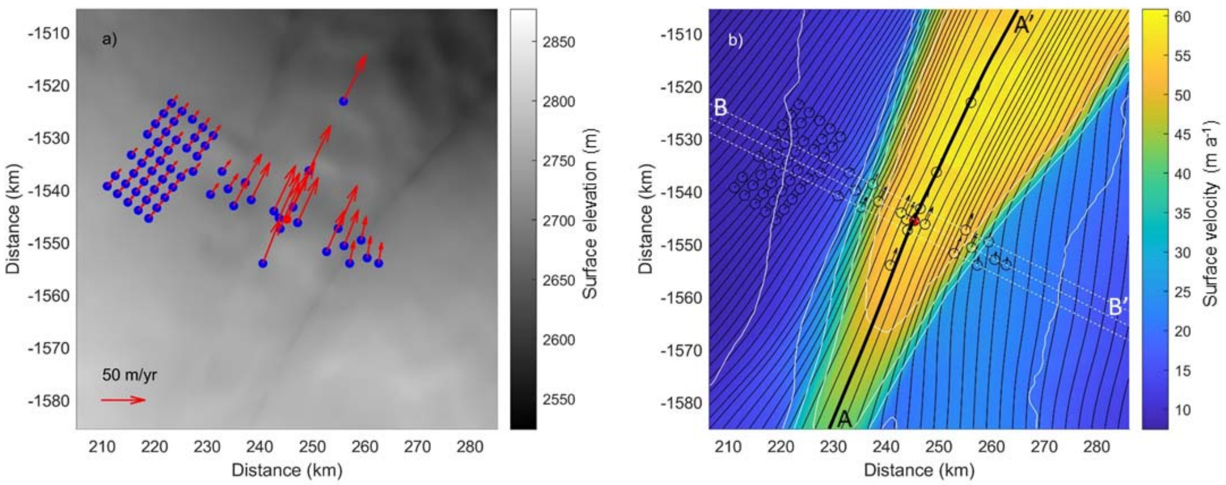

Figure 2. Maps of a 80 km x 80 km area around the EastGRIP site showing the GPS stake network (blue dots/circles), the central reference stake at the EastGRIP site (red dot), and the GPS derived surface velocities (red/black arrows) on an underlying map of: a) detailed surface elevation map (in meters) from ArcticDEM (Porter et al., 2018)) with a velocity scale bar, and b) MEaSUREs multi-year Greenland Ice Sheet Velocity v1 product (in m a^{-1}) (Joughin et al., 2016, 2017) with velocity contours and flow lines. The central flow line through EastGRIP is marked (black line). Ice flow and surface elevations along the central flow line A A' (black) and the three transverse lines B B' (white) are shown in Figs. 3 and 4, respectively. Figure 8 shows additional maps of the area.

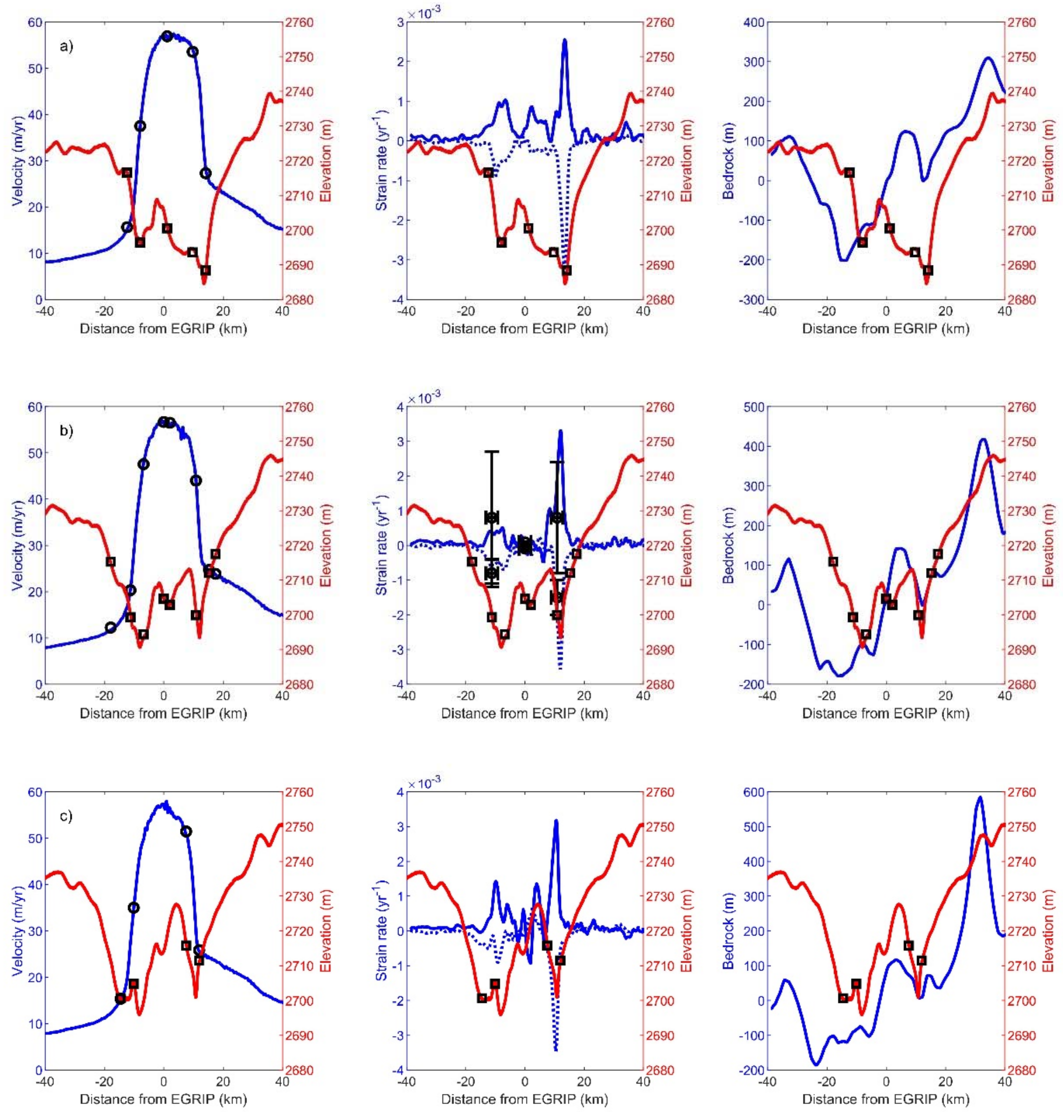
a)
b)
c)
Velocity (m/yr)
Strain rate (yr^{-1})
Bedrock (m)
Elevation (m)
Distance from EGRIP (km)
$\times 10^{-3}$

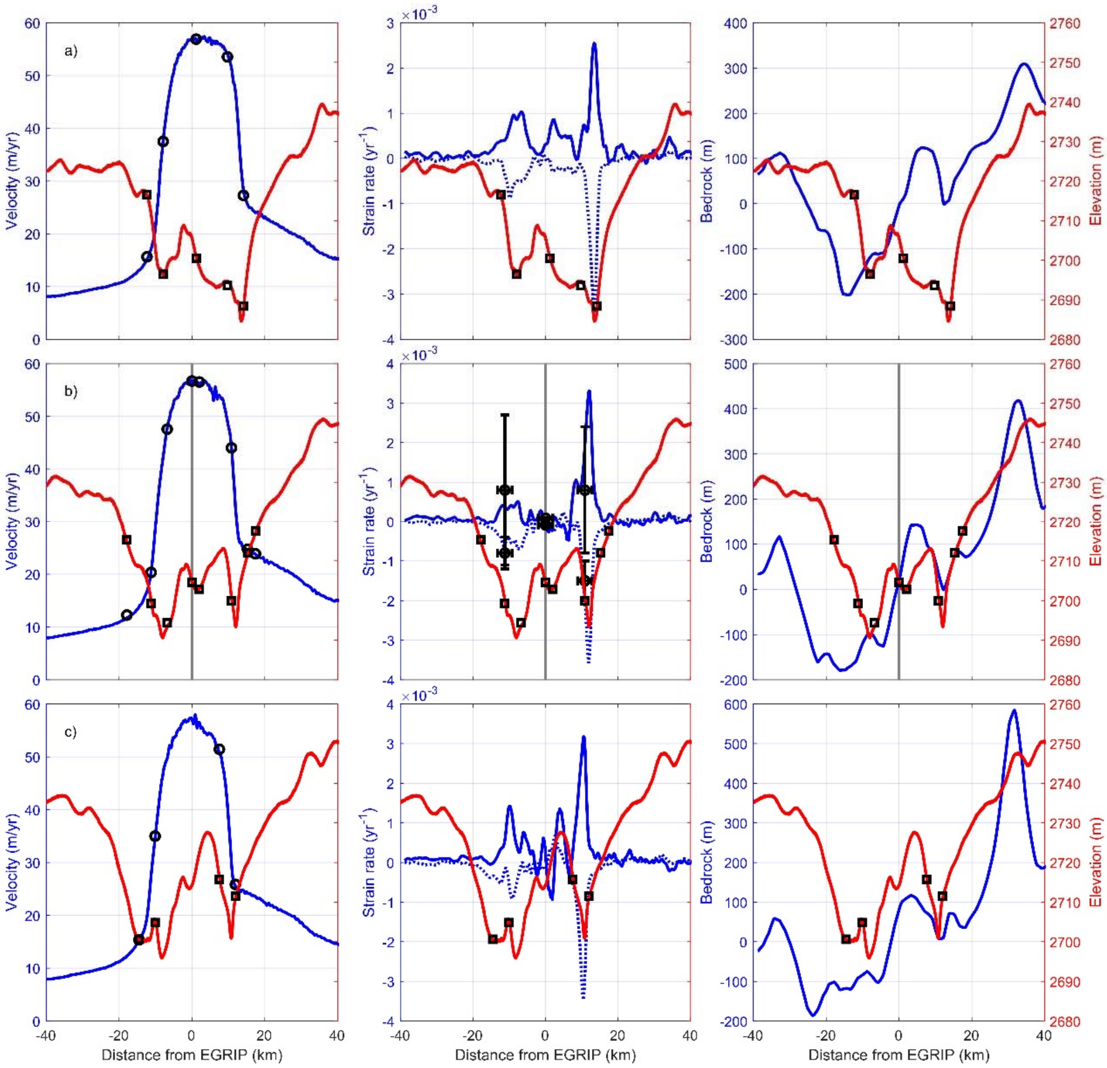

Figure 3. Ice flow and surface elevations of three cross sections of NEGIS separated by 2.5 km: a) downstream from the EastGRIP site, b) at the EastGRIP site, and c) upstream from the EastGRIP site (the cross sections are indicated on Fig. 2b). For each cross section, the three plots are: Left: Surface velocity (blue) and surface elevation (red). Middle: surface strain rates~~, longitudinal and transverse~~ relative to the local flow direction, along flow (blue full) and transverse to flow (blue ~~/~~dotted) with positive for stretching and negative for compression, and surface elevation (red). Right: Surface elevation (red) and bedrock topography (blue). GPS observations are shown as black circles/squares at three stakes marked in Fig. 5. Surface elevation is from the ArcticDEM (Porter et al., 2018), surface velocity and strain rate profiles are derived from MEaSUREs multi-year Greenland Ice sheet velocity v1 product (Joughin et al., 2016, 2017), and the bedrock topography is from BedMachine v3 (Morlighem et al., 2017a, 2017b). The vertical gray lines in b) panels indicate the position of the central stake near the EastGRIP site.

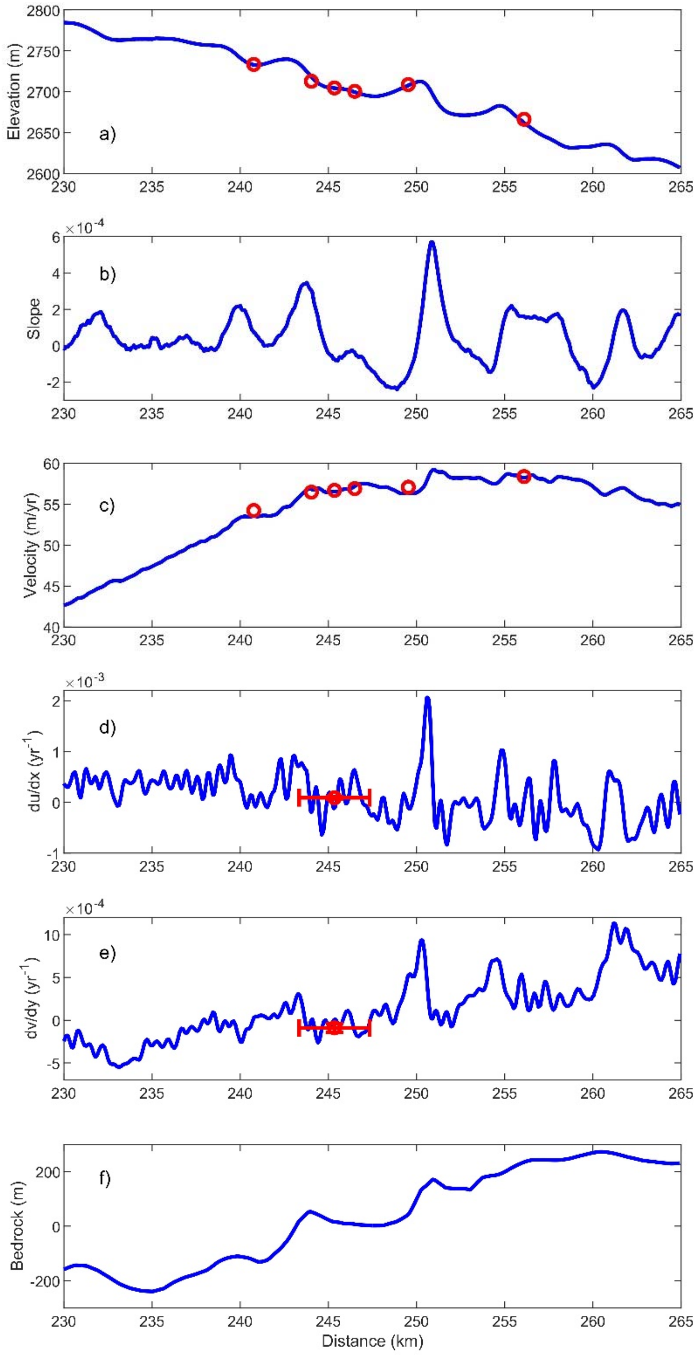
2800
2750
2700
2650
2600
Elevation (m)
a)
230
235
240
245
250
255
260
265
×10^-4
6
4
2
0
-2
Slope
b)
60
55
50
45
40
Velocity (m/yr)
c)
×10^-3
2
1
0
-1
du/dx (yr^-1)
d)
×10^-4
10
5
0
-5
dv/dy (yr^-1)
e)
200
0
-200
Bedrock (m)
f)
Distance (km)

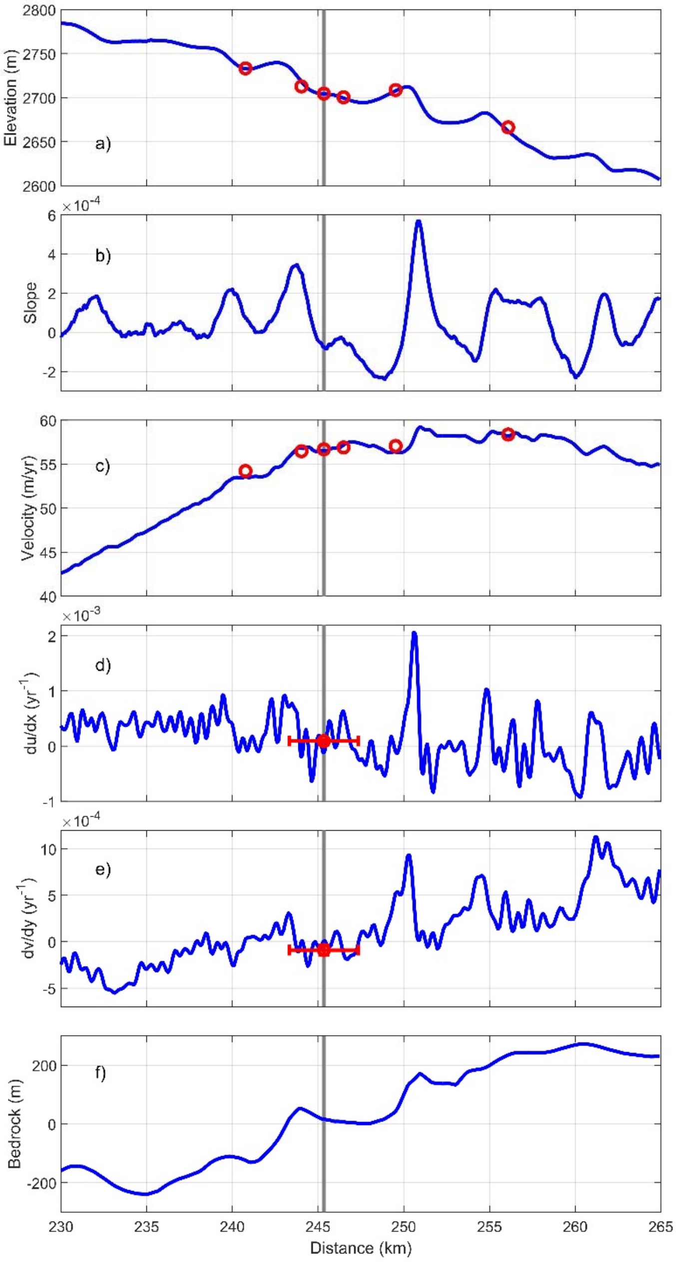

Figure 4. Variations along the central flowline of a) Surface elevation, b) surface slope, c) surface velocity, d) longitudinal strain rate $\dot{\epsilon}_{x'} = \partial u'/\partial x'$, e) transverse strain rate $\dot{\epsilon}_{y'} = \partial v'/\partial y'$, where prime indicates coordinates along and transverse to the flowline, and f) bedrock topography. The profiles in blue are derived from the ArcticDEM (Porter et al., 2018), MEaSUREs multi-year Greenland Ice Sheet Velocity v1 product (Joughin et al., 2016, 2017), and BedMachine v3 (Morlighem et al., 2017a, 2017b). GPS derived surface elevations, velocities and strain rates are shown in red. The vertical gray line indicates the position of the central stake near the EastGRIP site.

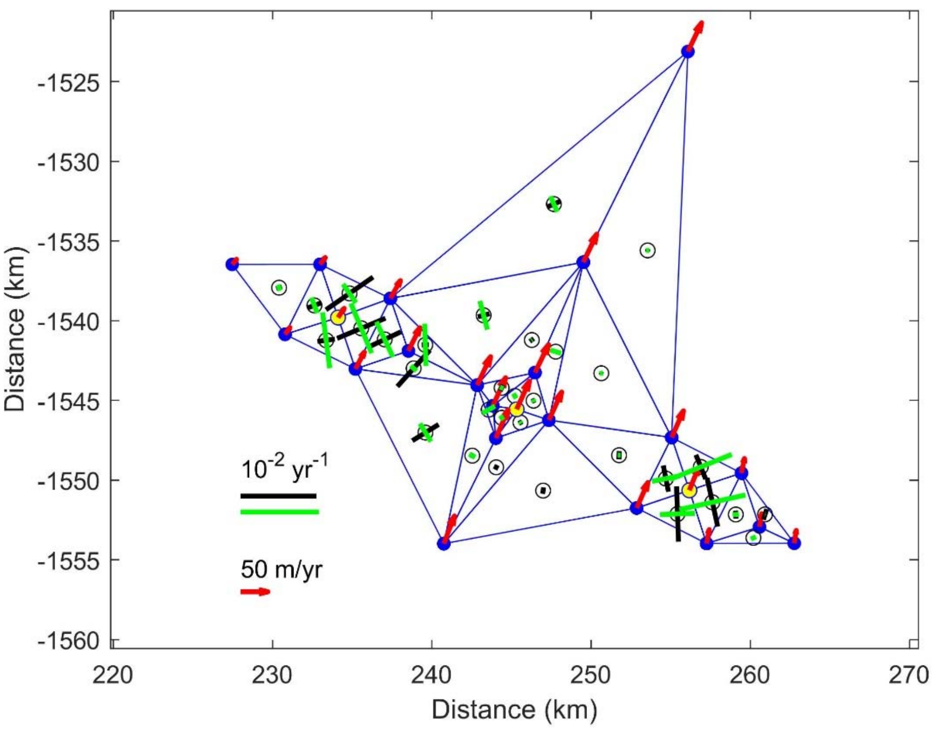

Figure 5. Horizontal principal strain rates for 32 different triangular sections within the GPS array. The principal strain rates are plotted at the centroids of each triangle (black circles) with black lines indicating positive strain rates (extension) and green lines indicating negative strain rates (compression). The GPS-derived surface velocities (red arrows) are plotted at the stakes (blue dots). At three GPS stakes (yellow dots), strain rates along the direction of the flow are calculated, see Fig. 3 (yellow dots).

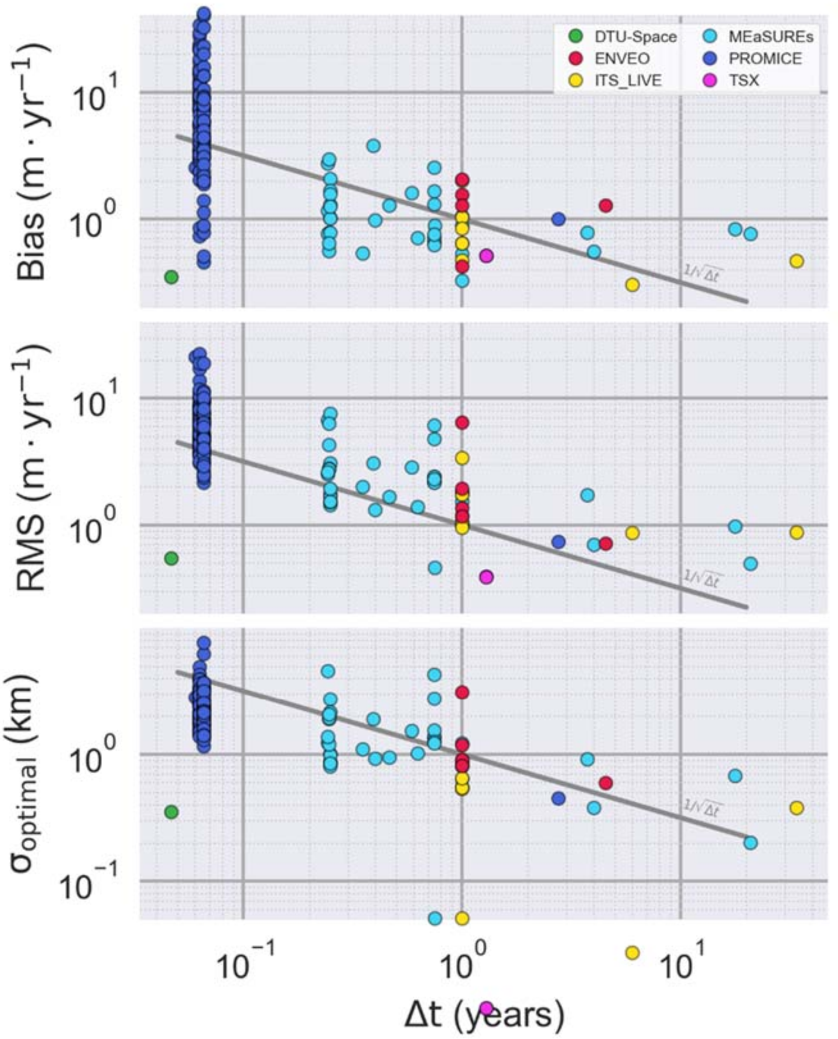
DTU-Space
ENVEO
ITS_LIVE
MEaSUREs
PROMICE
TSX
Bias (m · yr⁻¹)
RMS (m · yr⁻¹)
σ optimal (km)
1/√Δt
Δt (years)

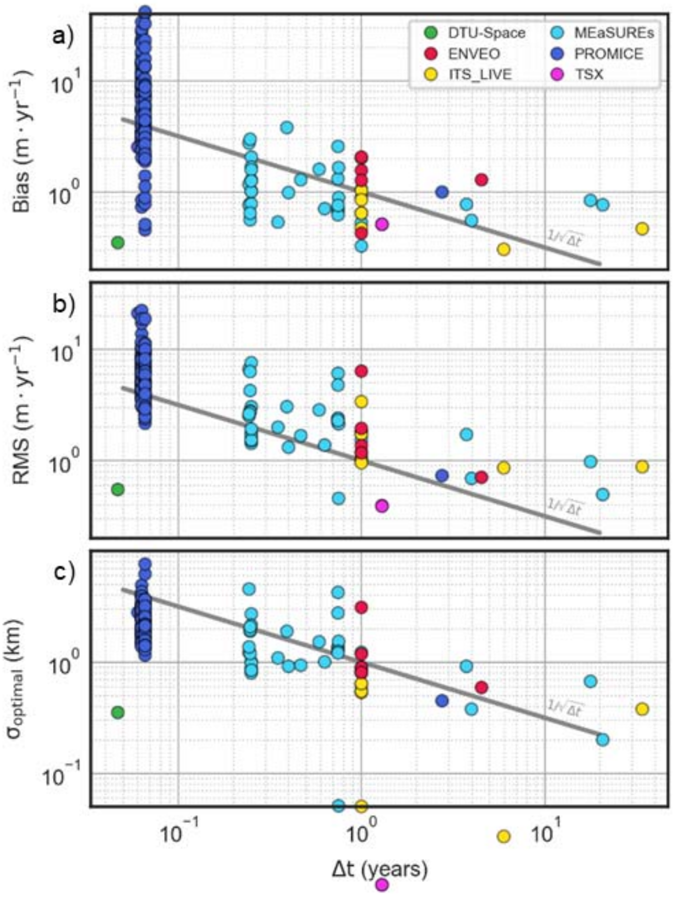

Figure 6. Results of the assessment of a list of 165 satellite-derived surface velocity products: a)~~. All results are shown as a function of Δt, the timespan of the velocity product.~~ ~~The top panel shows the~~ The mean bias of the velocity product compared to the GPS derived velocities at the location of the GPS poles, b)~~the middle panel shows~~ the standard deviation of the velocity products relative to GPS derived velocities (RMS), and c)~~the bottom panel shows~~ the optimal smoothing length of the velocity product that minimizes the standard deviation (σ). All results are shown as a function of Δt, the timespan of the velocity product. Notice that some products have been averaged over time to provide results with longer temporal coverage. The gray lines suggest a linear dependency of the bias, RMS and σ on temporal coverage Δt.

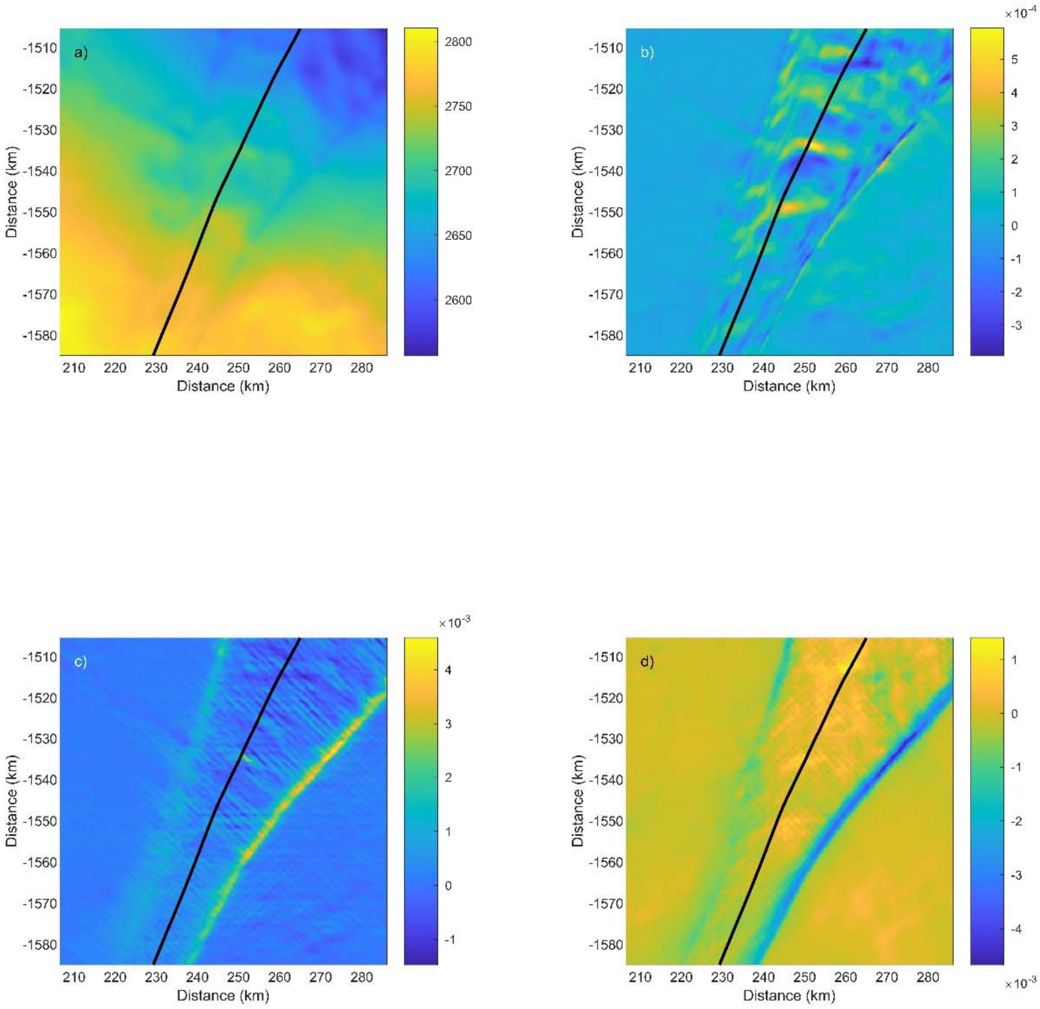

Figure 7. Maps of the 80 km x 80km section from Fig. 2 with the central flow line marked: a) surface elevation in meters, b) surface slope (dimensionless), both derived from the ArcticDEM (Porter et al., 2018), c) longitudinal strain rate $\dot{\epsilon}_{xt}$ in a^{-1} along the direction of the flow, and d) transverse strain rate $\dot{\epsilon}_{yt}$ in a^{-1} along the transverse direction to the flow, both from MEaSUREs multi-year Greenland Ice Sheet Velocity v1 product (Joughin et al., 2016, 2017).

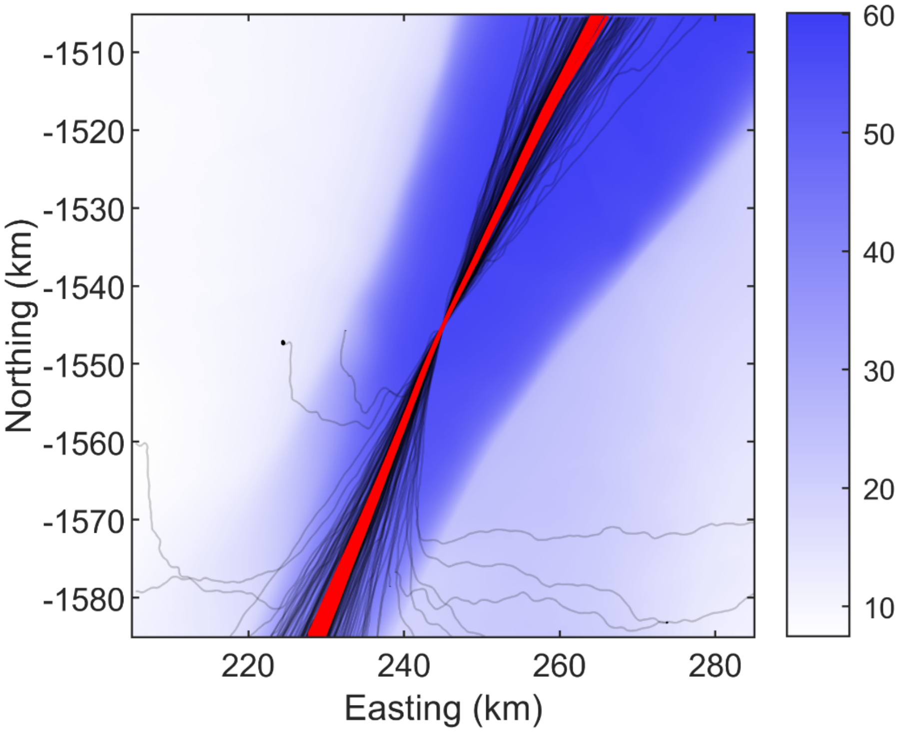

-1510
-1520
-1530
-1540
-1550
-1560
-1570
-1580
Northing (km)
220
240
260
280
Easting (km)
60
50
40
30
20
10

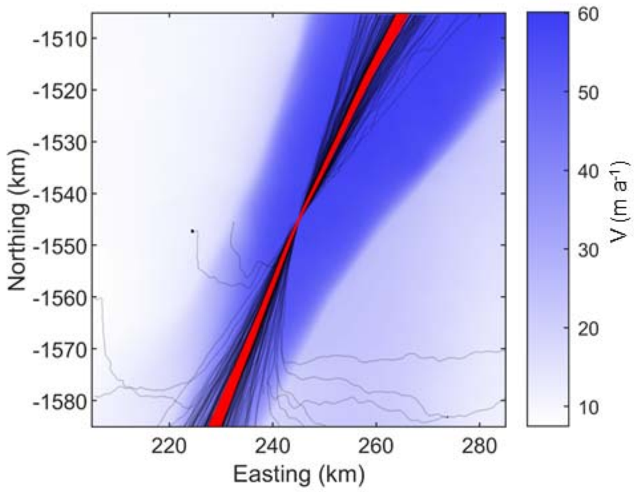

Figure ~~8~~7. Flowlines through the EastGRIP site (center of plot) calculated from the satellite derived velocity products. The line thickness depends on the bias of the product, with thick lines having a small bias and vice versa. The top four products with smallest bias are marked with red.

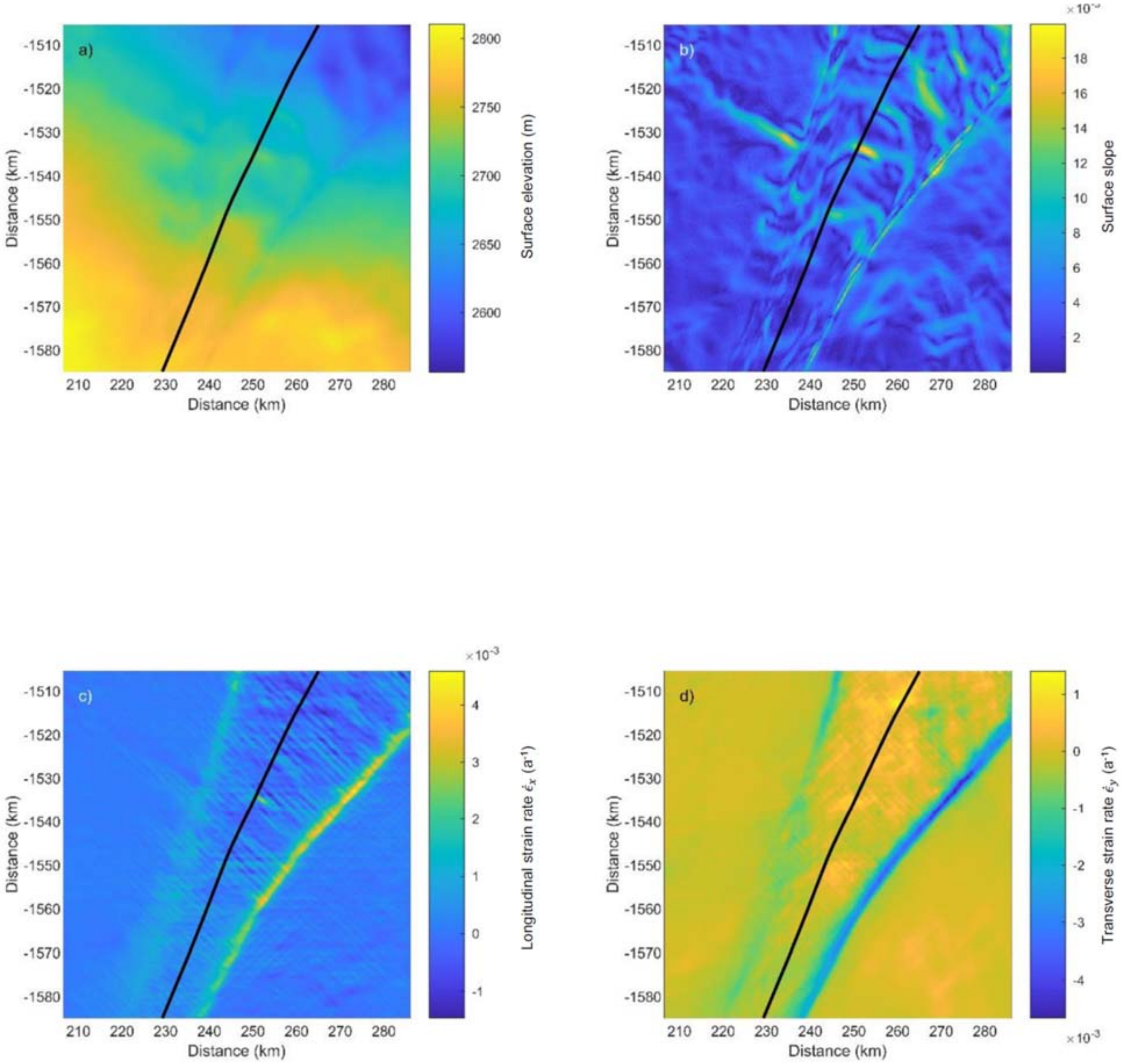

Figure 8. Maps of the 80 km x 80km section from Fig. 2 with the central flow line marked: a) surface elevation in meters, b) surface slope (dimensionless), both derived from the ArcticDEM (Porter et al., 2018), c) longitudinal strain rate $\dot{\epsilon}_{x'}$ in a^{-1} along the direction of the flow, and d) transverse strain rate $\dot{\epsilon}_{y'}$ in a^{-1} along the transverse direction to the flow, both from MEaSUREs multi-year Greenland Ice Sheet Velocity v1 product (Joughin et al., 2016, 2017).